# Abstract

This mathematics project is into the motion of pendulums. We begin the study with a simple pendulum and discussion about the motion. The project continues by deriving the equations of motion for the double pendulum, and a study of the motion governed by these equations. Here we introduce the idea of quasiperiodic motion. The project then tackles the system when the pivot vibrates, and we show the pendulum can be maintained in an 'upside-down' position with this vibration. We then continue with a mathematical analysis of this unusual stability.

# The Motion of a Pendulum

**Danny Hoskin**

**BSc (Hons) Mathematical Sciences**

**Contents**

# 1. Introduction

The pendulum is a tool that mathematicians and physicists have been using for many centuries to understand motion. It forms the foundation for much of the understanding that we have today of modern dynamics. Although the pendulum has been studied for such a long period of time it is still able to surprise many with its remarkable properties. For instance in 1908 Andrew Stephenson, from Manchester University, demonstrated how a pendulum could be made to stand upside down by vibrating the pivot vertically. Then in 1995 David Acheson and Tom Mullin appeared on television demonstrating the same trick for a triple pendulum, claiming that it was possible (in theory anyway) to make any number of connected pendulums stand in the inverted position.

**Project aims**

For this project I intend to start by looking at the motion of a simple pendulum and try to understand how the motion is achieved, and what affects the motion. I intend to look at the effects of damping on the pendulum, and plot graphs showing the displacement of a pendulum with respect to time. Early in the report I intend to use a couple of different numerical techniques to solve the equations of motion, and find which is better suited to this application. The techniques that I initially chose were Euler's Method and Improved Euler's Method, but after embarking on the project these become replaced with the classical fourth order Runge Kutta method. The reason for this change is the accuracy of the method (which I remark upon later in the report).

The project will then proceed to set up the equations of motion for the double pendulum. These will then be solved numerically using the Runge Kutta method. Again I plan to plot the motion of a double pendulum. When two masses are coupled together, such as the double pendulum, there can be transference of energy between the two masses; this is an effect I wish to show by creating formulae for the energy of each mass and plotting graphs showing the energy transference.

When I have the equations of motion for both the single and double pendulum, I wish to show how (in theory) the inverted state can be achieved. I will then look in-depth at the mathematical reasoning for this non-intuitive motion.

To solve the equations by numerical techniques I initially used Microsoft EXCEL, but MAPLE more predominantly since starting the project. I also plan to create a working demonstration of a double pendulum in MAPLE, using the fact that graphs can be animated with respect to time using MAPLE's animation functions. All the EXCEL and MAPEL worksheets will be saved on disk and will accompany the report, so the reader will be able to access them and change the variables to see the motion of the pendulums for themselves.

**Background research**

I discovered the idea of an inverted pendulum in a book entitled *From Calculus to Chaos*, (1997) by David Acheson. He talks of the research by Stephenson (1908), and his own experiments. In the book he refers to an episode of *Tomorrow's World* (October 1995) in which he demonstrates the inverted triple pendulum. I have been in touch with the BBC and they have sent me a copy of the episode, which I have watched with great interest. I have also bought a book Hannah and Miller entitled *Applied Mechanics* (1995), which gives useful background in analysing dynamical systems. Nicolas Rott describes about coupling effects in the paper mentioned in the bibliography (1970). A more detailed review of the above sources was given in the Initial Report for this project and is included in the Appendix section of this report (A1). A list of all the sources I have used is completed at the end of this report.

**Mathematical background**

A list of prior mathematical knowledge is listed below that would enable the reader to follow this report more easily. For sections 2, 3 and 4:

- Mechanics of a simple pendulum for small angles.
- Derivation of equations of motion using vector integrals and force balance laws.
- Phase diagrams to portray pendulum motion.
- Numerical techniques; Euler's method, Improved Euler's method, and Runge Kutta methods.

And then later, in section 5;

- Parametric resonance and stability of the Mathieu equation
- Basic Fourier series approximations

# 2. The Simple Pendulum

## 2.1 Equations of motion for a simple pendulum

The simple pendulum consists of a bob on the end of a string or wire that is attached to a fixed pivot. Figure 2.1 shows a diagram of a simple pendulum.

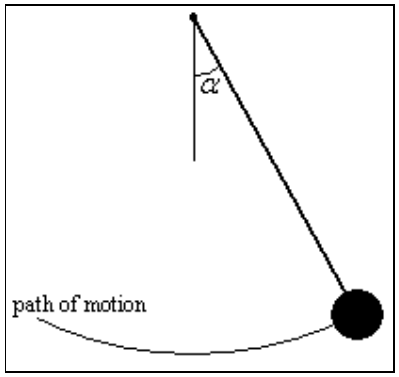


Figure 2.1. Diagram showing a simple pendulum, $\alpha$ denotes the angle between the string and the vertical.

For the duration of this project; $\alpha$ will denote the angle (in radians) between the string and vertical, $l$ the length (in metres) of the string, $m$ the mass (in kilograms) of the bob, $g$ acceleration (in meters per second squared) due to gravity, and $r$, $v$, and $a$ the displacement (in meters), velocity (in metres per second) and acceleration (in metres per second squared) of the bob respectively, $t$ will denote the time (in seconds) of motion.

As the pendulum moves through an angle ($\alpha$), the displacement can be give by the formula:

$$\text{Arc length} = l\alpha \tag{2.1}$$

$$\Rightarrow r = l\alpha. \tag{2.2}$$

From here we can say

$$v = -l\frac{d\alpha}{dt}. \tag{2.3}$$

The negative sign is included because as the angle increases the velocity decreases. This implies that

$$a = \frac{dv}{dt} = -l\frac{d^2\alpha}{dt^2}. \tag{2.4}$$

If we neglect any type of damping on the system then the only force acting on the pendulum (in the direction of travel and normal to the tension forces) is due to gravity. This force acts in the vertical direction, hence if $F$ denotes the total forces (in the direction of travel) acting upon the pendulum:

$$F = mg\sin(\alpha). \tag{2.5}$$

From Newton's laws of motion we are told that the total forces acting on an object is equal to its mass multiplied by its acceleration (for constant mass), i.e.

$$F = ma \tag{2.6}$$

$$\Rightarrow mg\sin(\alpha) = -ml\frac{d^2\alpha}{dt^2} \tag{2.7}$$

$$\Rightarrow \frac{d^2\alpha}{dt^2} + \frac{g}{l}\sin(\alpha) = 0. \tag{2.8}$$

Equation (2.8) is the equation of motion for a simple pendulum with no damping. Note that only the length of the string affects the motion of the pendulum and not the mass, so in theory a 2kg bob will swing the same as a 200kg bob.

We can simplify equation (2.8) letting

$$c^2 = \frac{g}{l}. \tag{2.9}$$

Hence equation (2.8) becomes

$$\frac{d^2\alpha}{dt^2} + c^2 \sin(\alpha) = 0. \tag{2.10}$$

However, in reality there is damping in the system due to air resistance. When a person rides a bike they feel more air against them the faster they go which means that air resistance varies according to how fast the person or object is moving. We will take the damping on the pendulum to be proportional to its velocity. If we add the damping into equation (2.10) then the equation of motion for a pendulum becomes

$$\frac{d^2\alpha}{dt^2} + k\frac{d\alpha}{dt} + c^2 \sin(\alpha) = 0, \tag{2.11}$$

where $k$ is the constant of proportionality. Notice that equations (2.10) and (2.11) are both second-order nonlinear differential equations.

**2.2 Solving the equation of motion for an undamped pendulum (small angles)**

The equation of motion for a pendulum that is not subject to damping is

$$\frac{d^2\alpha}{dt^2} + c^2 \sin(\alpha) = 0. \tag{2.12}$$

For small values of α

$$\sin(\alpha) \approx \alpha. \tag{2.13}$$

Hence (2.12) is approximated by

$$\frac{d^2\alpha}{dt^2} + c^2\alpha = 0, \quad \text{for } \alpha \text{ small.} \tag{2.14}$$

Equation (2.14) is a second order differential equation with a solution of the form

$$\alpha(t) = A\cos(ct) + B\sin(ct), \tag{2.15}$$

where $A$ and $B$ are constants depending on the initial conditions. If we allow $\alpha_0$ to represent the initial angle that the pendulum formed with the vertical, and $u$ the initial angular velocity of the pendulum, then

$$\alpha_0 = A\cos(0) + B\sin(0), \quad \text{and} \quad u = -cA\sin(0) + cB\cos(0), \tag{2.16}$$

$$\Rightarrow \qquad A = \alpha_0, \qquad \text{and} \qquad B = \frac{u}{c}, \tag{2.17}$$

$$\Rightarrow \alpha(t) = \alpha_0\cos(ct) + \frac{u}{c}\sin(ct). \tag{2.18}$$

In most cases the pendulum will be released at rest from a certain angle $(\alpha_0)$, in this instance (2.18) becomes

$$\alpha(t) = \alpha_0\cos(ct). \tag{2.19}$$

From equation (2.19) we can see that, with no resistance the pendulum will always return to its original height, with amplitude of $\alpha_0$. From the 'swinging' motion of the pendulum we expect the motion to be that of a perfect cosine wave. Figure 2.2a shows graphically how the angles changes as time changes. To create the graphic, the pendulum was given an initial angle of $0.2^c$ and the length of the string was scaled such that $c = 1$.

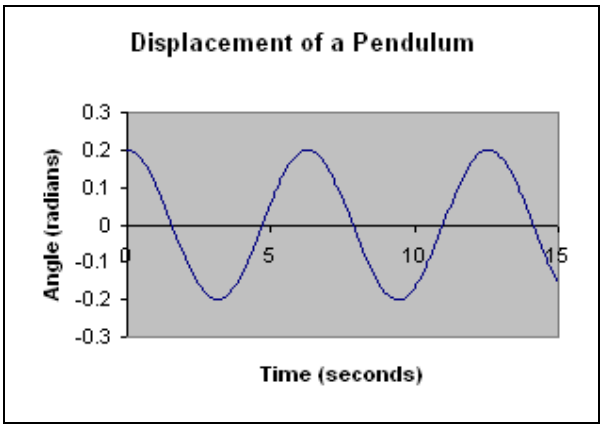


Figure 2.2a. An example of the displacement of a simple pendulum that is undamped.

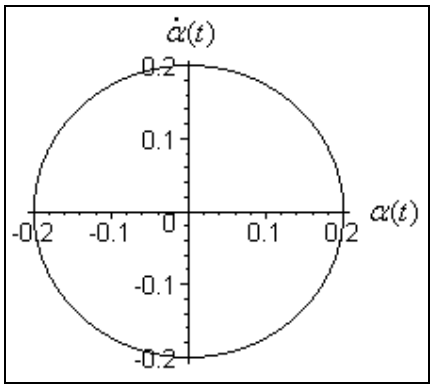


Figure 2.2b. The phase plane of a simple pendulum.

Figure 2.2b gives another interpretation of the motion. It shows us that, as we assumed before, that as the angle decreases the speed increases until the angle is zero (the bob is directly under the pivot), then as the bob then swings away from the pivot the speed then starts to decrease until the bob is at its maximum swing. This is the type of motion we see from a pendulum. The phase plane is significant in this instance because it is a closed circle. It tells us that the pendulum is swinging in simple harmonic motion; that is it keeps swinging to and from the same points (with the same frequency) for all of time. We defined the maximum angle implicitly when we gave the pendulum an initial angle, the pendulums angle decreases immediately after it is

let go, hence that initial angle was the maximum, this is why the phase plane has a radius of 0.2.

From equation (2.19) we can see that the fundamental period of the pendulum (time taken to swing from certain point and back again) is

$$2\pi\sqrt{\frac{l}{g}}. \tag{2.20}$$

Hence the period is proportional to $\sqrt{l}$ , and independent of $\beta$ (the amplitude), Galileo observed this in observations in 1602. This means that no mater the initial angle the pendulum will always swing with the same period.

Simple harmonic motion is a periodic motion that always accelerates to a fixed point in its path (in our case the pendulums position when at rest), and the acceleration is proportional to its distance from the fixed point (this is shown in equation 2.14). Hence, Figure 2.2 is a perfect example of simple harmonic motion.

**2.3 Solving the equation of motion for an undamped pendulum (all angles)**

While it is useful to approximate (2.13) for small angles of displacement, we also need to consider the problem for larger angles. We start from equation (2.10)

$$\frac{d^2\alpha}{dt^2} + c^2 \sin(\alpha) = 0. \tag{2.21}$$

In solving this equation I intend to compare two methods of numerically solving differential equations. Firstly we shall employ Euler's method. We need to express (2.21) as two first-order differential equations.

Let $$z = \frac{d\alpha}{dt}, \tag{2.22}$$

$$\Rightarrow \frac{dz}{dt} = \frac{d^2\alpha}{dt^2}. \tag{2.23}$$

By substituting (2.23) into (2.21) we arrive at the system of equations

$$\frac{dz}{dt} = -c^2 \sin(\alpha), \tag{2.24a}$$

$$\frac{d\alpha}{dt} = z. \tag{2.24b}$$

We can then apply Euler's method (see Jacques and Judd for examples of the method) to the above equations to plot the motion of the pendulum (the procedure is explicitly given in A2 of the Appendix). Figure 2.3 is a graphical representation of the process using the same initial conditions as those used to create Figure 2.2a.

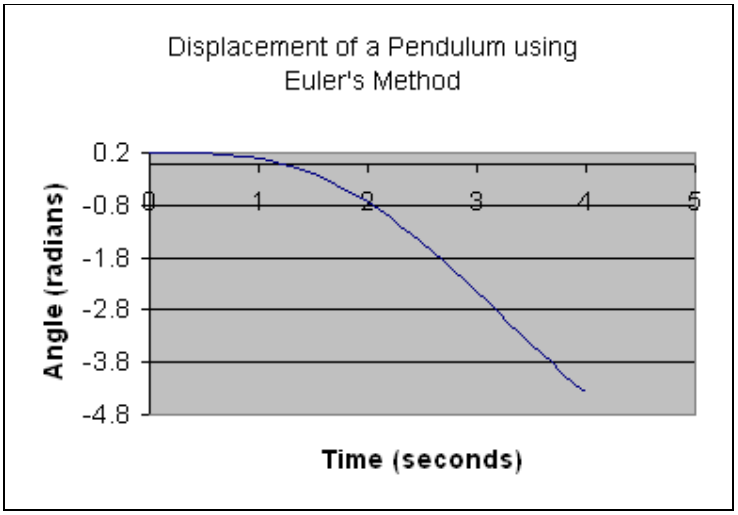


Figure 2.3. Motion of a pendulum solved numerically

by Euler's Method with a step size of 0.1.

We can see from Figure 2.3 that we have not obtained the same type motion as described by equation (2.19). This could suggest that Euler's method could not be suited to this problem. Let us check this…

We can implement Modified Euler's Method (the procedure is again shown in A2 of the Appendix, see Jacques and Colin Judd for examples of the method). This is an improved version of Euler's method. Figure 2.4 is a graphical interpretation of the Improved Euler's Method using the same conditions as those for Figure 2.3.

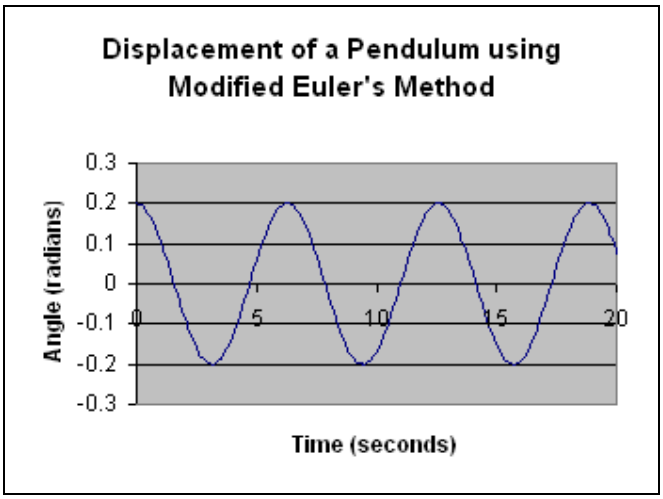


Figure 2.4. Motion of a pendulum solved numerically by Modified Euler's method.

We can see that Modified Euler's method gives a more accurate interpretation of the motion of the pendulum. This is to be expected because of the error terms involved in each method. The global error given by Euler's method is proportional to $h$ (where $h$ relates to the step size for the iterative schemes), where as this is $h^2$ for the Modified Euler's method. We could find better approximations for each by reducing the step

length (i.e. make *h* smaller), however there are fewer steps needed if we use a method of higher accuracy, so at this point we opt for the second method.

Figure 2.4 shows the pendulum swing to and fro exactly as the Figure 2.2a. (The phase plane is not included here as it is also the same as before). In fact if the graphs from both Figure 2.2a and 2.4 were superimposed upon each other they would appear as one graph. This is because we used a small initial angle for Figure 2.4. If the angle increases significantly then the graphs split apart and the model for small displacement gives inaccurate readings because the assumption of 'small' angles is no longer valid, Figure 2.5 demonstrates this.

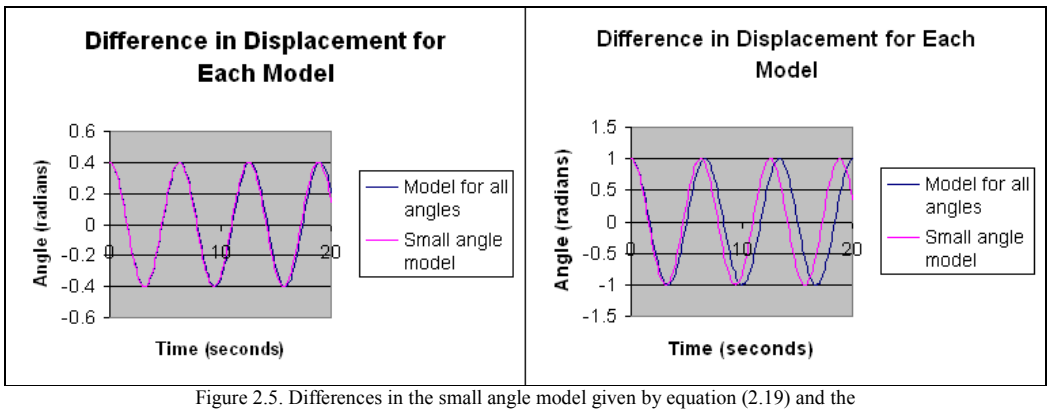


Figure 2.5. Differences in the small angle model given by equation (2.19) and the model for all angles given by set of equations (2.24).

The first graph of Figure 2.5 shows the two models starting to separate when the initial angle is $0.4^c$. The second show the large difference in the two methods when the initial angle is raised to $1^c$.

## 2.4 Solving the equations of motion for a damped pendulum

So far we have concentrated on the equation of motion (2.10), that of an undamped pendulum. Let us now turn our attention to the equation of motion (2.11), that of a pendulum experiencing damping. The equation of motion was found to be

$$\frac{d^2\alpha}{dt^2} + k\frac{d\alpha}{dt} + c^2 \sin(\alpha) = 0\,. \tag{2.25}$$

As before we need to convert (2.25) into a set of first-order differential equations. We do this by the same method as before, and the set becomes,

$$\frac{dz}{dt} = -kz - c^2 \sin(\alpha)\,, \tag{2.26a}$$

$$\frac{d\alpha}{dt} = z\,. \tag{2.26b}$$

Figure 2.6 shows a numerical solution of equations (2.26) obtained from Improved Euler's method, using the same initial conditions as used in Figures 2.2 and 2.4.

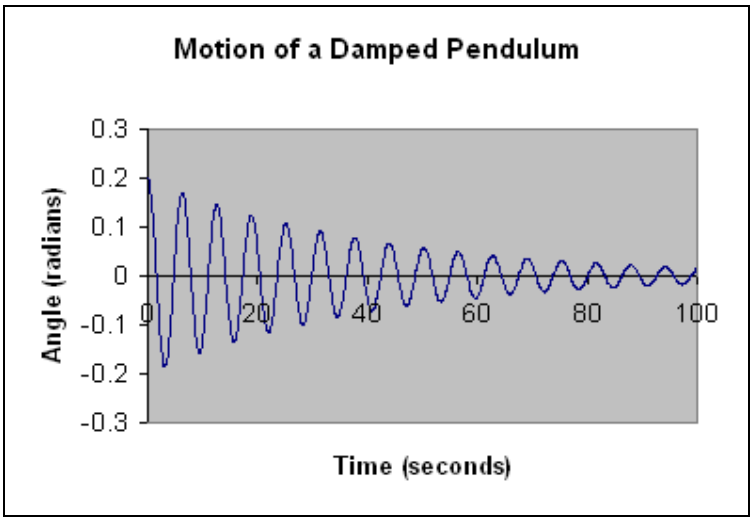


Figure 2.6a The motion of a damped pendulum with resistive force proportional to the speed of the pendulum.

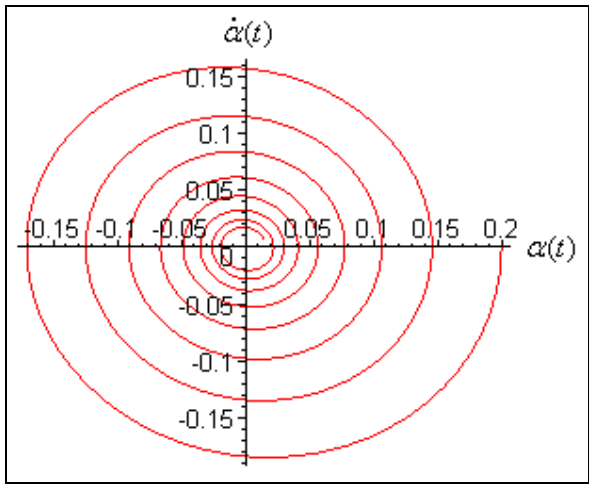


Figure 2.6b. The phase plane of the damped pendulum

For the example given in Figures 2.6, $k$ had to be defined. This was the constant that determined how *strong* the resistive force was. $k$ was chosen to be 0.1. We can see from Figure 2.6a how the amplitude decreases with time. The effect of damping forces the pendulum not to swing as high as it did on the previous swing. The phase plane is also more interesting this time. It is no longer closed but now spiralling into the centre because the maximum angle of each swing decreases, and hence also its maximum speed. The pendulum will carry on in this manner until it finally stops; this is how a pendulum appears in the real world. Note that because we have only modelled the motion and used a numerical scheme to solve this model our solution will never remain at zero for finite time, but will asymptotically approach zero.

Before we continue it may be of interest to see the path that is traced out by the mass on the $xy$-plane because this is how it appears in real life.

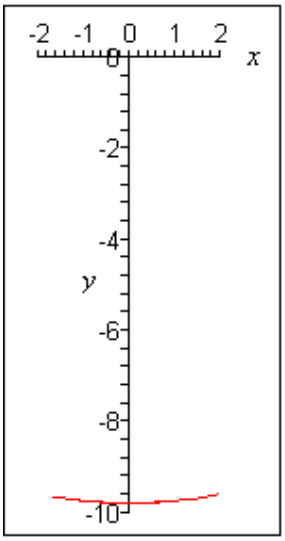


Figure 2.6c The path traced out by the pendulum

Figure 2.6c shows the path traced out from the pendulum from Figure 2.6b. The curve is what we would expect to see from a swinging pendulum, notice that the bob is confined to move on a circle.

In the initial report we looked at the affects of changing each of the parameters (rod length, initial angle, damping effect and step size for the numerical schemes). This section has been moved to A4 of the Appendix in order to have enough room in the report for the more advanced mathematics in later sections. Here we merely summarise the findings.

We find that when we shorten the length of the rod (which had the same effect as increasing the effect of gravity) this has the effect of shortening the period (of swing) of the pendulum. With a damping effect the amplitude of motion (related to the height of swing) is reduced. The higher the damping effect, the bigger effect of reducing this amplitude. Importantly the damping effect did not appear to affect the period. If we

increase the initial angle we find that the pendulum swings with the same period, but with lower amplitude. While looking at the step size we concluded that we required a more accurate numerical procedure. This is why all numerical calculations are performed using the classical Runge Kutta $4^{th}$ order scheme (Jacques and Judd page 254) in the remainder of this report.

# 3. The Double Pendulum

## 3.1 Deriving the equations of motion

The type of double pendulum we shall cover in this project is shown below.

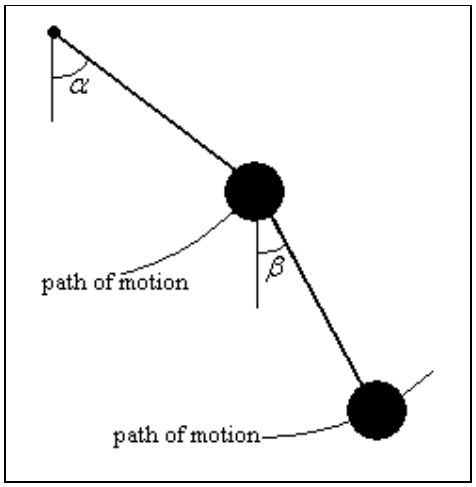


Figure 3.1 Diagram of a double pendulum.

The notation used in this section will be consistent with that used in the previous section. Let $l_1$ and $m_1$ denote the length of the string and mass respectively for the higher pendulum, and $l_2$ and $m_2$ correspondingly for the lower. The angles, $\alpha$ and $\beta$, are the angles between the strings and the vertical as shown.

The motion for a double pendulum is considerably more complicated than that of a simple pendulum. The equations of motion for the double pendulum are derived on the next page.

We shall start by considering the two masses as coordinates on the standard *xy*-plane. The origin shall be the fixed pivot to which the first rod is attached. As such the coordinates for each of the two masses can be shown to be

$$x_1 = l_1 \sin(\alpha), \tag{3.1a}$$
$$y_1 = -l_1 \cos(\alpha), \tag{3.1b}$$
$$x_2 = x_1 + l_2 \sin(\beta), \tag{3.1c}$$
$$y_2 = y_1 - l_2 \cos(\beta). \tag{3.1d}$$

Acceleration of each mass is given by the second derivative of (3.1) which leads to

$$\frac{d^2 x_1}{dt^2} = -l_1 \left( \frac{d\alpha}{dt} \right)^2 \sin(\alpha) + l_1 \frac{d^2 \alpha}{dt^2} \cos(\alpha), \tag{3.2a}$$
$$\frac{d^2 y_1}{dt^2} = l_1 \left( \frac{d\alpha}{dt} \right)^2 \cos(\alpha) + l_1 \frac{d^2 \alpha}{dt^2} \sin(\alpha), \tag{3.2b}$$
$$\frac{d^2 x_2}{dt^2} = \frac{d^2 x_1}{dt^2} - l_2 \left( \frac{d\beta}{dt} \right)^2 \sin(\beta) + l_2 \frac{d^2 \beta}{dt^2} \cos(\beta), \tag{3.2c}$$
$$\frac{d^2 y_2}{dt^2} = \frac{d^2 y_1}{dt^2} + l_2 \left( \frac{d\beta}{dt} \right)^2 \cos(\beta) + l_2 \frac{d^2 \beta}{dt^2} \sin(\beta). \tag{3.2d}$$

Let $T_1$ and $T_2$ define the tension in each of the respective rods. If we neglect air resistance, the total of the forces acting on $m_1$ in the horizontal direction are

$$T_2 \sin(\beta) - T_1 \sin(\alpha). \tag{3.3}$$

We can then use this in Newton's second law

$$F = ma, \tag{3.4}$$

to give

$$T_2 \sin(\beta) - T_1 \sin(\alpha) = m_1 \frac{d^2 x_1}{dt^2}. \tag{3.5a}$$

We then apply the same procedure to $m_1$ in the vertical direction, and to $m_2$ in both directions to give

$$T_1\cos(\alpha)-T_2\cos(\beta)-m_1g=m_1\frac{d^2y_1}{dt^2}, \tag{3.5b}$$

$$-T_2\sin(\beta)=m_2\frac{d^2x_2}{dt^2}, \tag{3.5c}$$

$$T_2\cos(\beta)-m_2g=m_2\frac{d^2y_2}{dt^2}. \tag{3.5d}$$

Substitute (3.5c) into (3.5a) and multiply the result by $\cos(\alpha)$ (and rearrange) to give

$$\left(-m_2\frac{d^2x_2}{dt^2}-m_1\frac{d^2x_1}{dt^2}\right)\cos(\alpha)=T_1\sin(\alpha)\cos(\alpha), \tag{3.6}$$

From (3.5d), we see that

$$T_2\cos(\beta)=m_2\frac{d^2y_2}{dt^2}+m_2g. \tag{3.7}$$

If we substitute (3.7) into (3.5b) and multiply the result by $\sin(\alpha)$ (and rearrange), we get

$$T_1\cos(\alpha)\sin(\alpha)=\left(m_2\frac{d^2y_2}{dt^2}+m_2g+m_1g+m_1\frac{d^2y_1}{dt^2}\right)\sin(\alpha). \tag{3.8}$$

Hence if we equate (3.6) and (3.8) we get

$$-\left(m_2\frac{d^2x_2}{dt^2}+m_1\frac{d^2x_1}{dt^2}\right)\cos(\alpha)=\left(m_2\frac{d^2y_2}{dt^2}+m_2g+m_1g+m_1\frac{d^2y_1}{dt^2}\right)\sin(\alpha). \tag{3.9}$$

Substitute set of equations (3.2) into equation (3.9) and simplify to obtain,

$$\begin{aligned}&\frac{d^2\alpha}{dt^2}l_1(m_1+m_2)-\left(\frac{d\beta}{dt}\right)^2l_2m_2\sin(\beta-\alpha)\\&+\frac{d^2\beta}{dt^2}m_2l_2\cos(\beta-\alpha)+(m_1+m_2)g\sin(\alpha)=0.\end{aligned} \tag{3.10}$$

Multiply (3.5c) by $\cos(\beta)$, and multiply (3.5d) by $\sin(\beta)$ and equate the result to give,

$$-\frac{d^2x_2}{dt^2}\cos(\beta)=\left(\frac{d^2y_2}{dt^2}+g\right)\sin(\beta). \tag{3.11}$$

Substituting set of equations (3.2) into (3.11) (and simplifying) gives,

$$l_2 \frac{d^2\beta}{dt^2} + l_1 \frac{d^2\alpha}{dt^2}\cos(\beta-\alpha) + l_1\left(\frac{d\alpha}{dt}\right)^2 \sin(\beta-\alpha) + g\sin(\beta) = 0\,. \qquad (3.12)$$

We can the simplify further if we define

$$m = \frac{m_2}{m_1 + m_2}\ . \qquad (3.13)$$

Hence (3.10) becomes

$$l_1 \frac{d^2\alpha}{dt^2} + ml_2 \frac{d^2\beta}{dt^2}\cos(\beta-\alpha) - ml_2\left(\frac{d\beta}{dt}\right)^2 \sin(\beta-\alpha) + g\sin(\alpha) = 0\,. \quad (3.14)$$

Thus the equations of motion for a double pendulum are

$$l_1 \frac{d^2\alpha}{dt^2} + ml_2 \frac{d^2\beta}{dt^2}\cos(\beta-\alpha) - ml_2\left(\frac{d\beta}{dt}\right)^2 \sin(\beta-\alpha) + g\sin(\alpha) = 0\,, \quad (3.15a)$$

$$l_2 \frac{d^2\beta}{dt^2} + l_1 \frac{d^2\alpha}{dt^2}\cos(\beta-\alpha) + l_1\left(\frac{d\alpha}{dt}\right)^2 \sin(\beta-\alpha) + g\sin(\beta) = 0\,, \qquad (3.15b)$$

where

$$m = \frac{m_2}{m_1 + m_2}\,. \qquad (3.15c)$$

### 3.2 Motion at small angles of displacement

The equations of motion as described by the system of equations (3.15) are very complex to solve, even numerically, so let us begin by placing some restrictions on our system to simplify these equations. Firstly, let us assume that both strings (or rods) are the same length, *l*. i.e.

$$l_1 = l_2 = l\,. \tag{3.16}$$

Secondly, let us study the system for only small displacements. Hence

$$\sin(\beta - \alpha) \to \beta - \alpha\,. \tag{3.17}$$

Also

$$\sin(\alpha) \approx \alpha\,, \tag{3.18a}$$

and

$$\sin(\beta) \approx \beta\,. \tag{3.18b}$$

If we then substitute these simplifications into the system of equations (3.15), and look only at the leading order terms we find

$$\frac{d^2\alpha}{dt^2} + m\frac{d^2\beta}{dt^2} + \frac{g}{l}\alpha = 0\,, \tag{3.19a}$$

$$\frac{d^2\beta}{dt^2} + \frac{d^2\alpha}{dt^2} + \frac{g}{l}\beta = 0\,, \tag{3.19b}$$

where

$$m = \frac{m_2}{m_1 + m_2}\,. \tag{3.19c}$$

Hence, the system of equations given by (3.19) describes the motion of a double pendulum with equal length strings for small displacements.

### 3.3 Solving the equations of motion at small displacement angles

To solve the equations of motion for the double pendulum at small angles of displacement, we firstly need to rewrite the set of equation (3.19) as a series of first order differential equations. We shall define the variables $\lambda$ and $\mu$ as

$$\mu = \frac{d\alpha}{dt}, \qquad \text{(3.20a)} \qquad \text{and} \qquad \lambda = \frac{d\beta}{dt}, \qquad \text{(3.20b)}$$

Our system of first order differential equations (for equations (3.19)) becomes,

$$\frac{d\alpha}{dt} = \mu, \qquad \text{(3.21a)}$$

$$\frac{d\beta}{dt} = \lambda, \qquad \text{(3.21b)}$$

$$\frac{d\lambda}{dt} = \frac{(\beta - \alpha)}{(m-1)} c^2, \qquad \text{(3.21c)}$$

$$\frac{d\mu}{dt} = \frac{(\alpha - m\beta)}{(m-1)} c^2. \qquad \text{(3.21d)}$$

where we have reintroduced $c^2 = g/l$ as we did in section 2.

Because all the variables on the right-hand side of (3.21) are first order we can solve this system explicitly as an eigenvalue problem.

If we let $N = \frac{c^2}{(1-m)}$, then the set of equations (3.21) can be expressed as,

$$\begin{bmatrix} \dot{\alpha} \\ \dot{\beta} \\ \dot{\lambda} \\ \dot{\mu} \end{bmatrix} = \begin{bmatrix} 0 & 0 & 0 & 1 \\ 0 & 0 & 1 & 0 \\ N & -N & 0 & 0 \\ -N & mN & 0 & 0 \end{bmatrix} \begin{bmatrix} \alpha \\ \beta \\ \lambda \\ \mu \end{bmatrix} \qquad (3.22)$$

We have four eigenvalues/eigenvectors for the coefficient matrix in (3.22). The eigenvalues and the corresponding eigenvectors are shown below,

| Eigenvalue | Eigenvector |
|---|---|
| $\sqrt{-N-N\sqrt{m}}$ | $\begin{bmatrix} -\sqrt{m} \\ 1 \\ \sqrt{-N-N\sqrt{m}} \\ -\sqrt{m}\sqrt{-N-N\sqrt{m}} \end{bmatrix}$ |
| $-\sqrt{-N-N\sqrt{m}}$ | $\begin{bmatrix} -\sqrt{m} \\ 1 \\ -\sqrt{-N-N\sqrt{m}} \\ \sqrt{m}\sqrt{-N-N\sqrt{m}} \end{bmatrix}$ |
| $\sqrt{-N+N\sqrt{m}}$ | $\begin{bmatrix} \sqrt{m} \\ 1 \\ \sqrt{-N+N\sqrt{m}} \\ \sqrt{m}\sqrt{-N+N\sqrt{m}} \end{bmatrix}$ |
| $-\sqrt{-N+N\sqrt{m}}$ | $\begin{bmatrix} \sqrt{m} \\ 1 \\ -\sqrt{-N+N\sqrt{m}} \\ -\sqrt{m}\sqrt{-N+N\sqrt{m}} \end{bmatrix}$ |

Since $0 < N$ (because $0 < m < 1$) the eigenvalues and eigenvectors are complex. Also we can see that these eigenvalues occur in complex conjugate pairs. We need only to use one of each of the pairs (MaQuarrie page 555), and there is a solution of the matrix system in (3.22) given in the form,

$$\mathbf{x}(t) = \begin{bmatrix} \alpha(t) \\ \beta(t) \\ \lambda(t) \\ \mu(t) \end{bmatrix} = \begin{bmatrix} -\sqrt{m} \\ 1 \\ ia \\ -i\sqrt{m}a \end{bmatrix} e^{iat} + \begin{bmatrix} \sqrt{m} \\ 1 \\ ib \\ i\sqrt{m}b \end{bmatrix} e^{ibt} \tag{3.23}$$

where $a = \sqrt{N + N\sqrt{m}}$ and $b = \sqrt{N - N\sqrt{m}}$ .

Using the fact that $e^{iat} = \cos(at) + i\sin(at)$ we can rewrite (3.23) as,

$$\mathbf{x}(t) = \begin{bmatrix} -\sqrt{m}\cos(at) \\ \cos(at) \\ -a\sin(at) \\ \sqrt{m}a\sin(at) \end{bmatrix} + i\begin{bmatrix} -\sqrt{m}\sin(at) \\ \sin(at) \\ a\cos(at) \\ -\sqrt{m}a\cos(at) \end{bmatrix} + \begin{bmatrix} \sqrt{m}\cos(bt) \\ \cos(bt) \\ -b\sin(bt) \\ -\sqrt{m}b\sin(bt) \end{bmatrix} + i\begin{bmatrix} \sqrt{m}\sin(bt) \\ \sin(bt) \\ b\cos(bt) \\ \sqrt{m}b\cos(bt) \end{bmatrix} \tag{3.24}$$

Each of the vectors on the right hand side of (3.24) is a linearly independent solution of the matrix system given in (3.22) (again see MaQuarrie page 555). Hence a general solution to the matrix problem is given by,

$$\mathbf{x}(t) = c_1\begin{bmatrix} -\sqrt{m}\cos(at) \\ \cos(at) \\ -a\sin(at) \\ \sqrt{m}a\sin(at) \end{bmatrix} + c_2\begin{bmatrix} -\sqrt{m}\sin(at) \\ \sin(at) \\ a\cos(at) \\ -\sqrt{m}a\cos(at) \end{bmatrix} + c_3\begin{bmatrix} \sqrt{m}\cos(bt) \\ \cos(bt) \\ -b\sin(bt) \\ -\sqrt{m}b\sin(bt) \end{bmatrix} + c_4\begin{bmatrix} \sqrt{m}\sin(bt) \\ \sin(bt) \\ b\cos(bt) \\ \sqrt{m}b\cos(bt) \end{bmatrix}$$

Given the initial conditions:

$$\mathbf{x}(0) = \begin{bmatrix} \alpha(0) \\ \beta(0) \\ \lambda(0) \\ \mu(0) \end{bmatrix} = \begin{bmatrix} \alpha_0 \\ \beta_0 \\ 0 \\ 0 \end{bmatrix}$$

we find,

$$\begin{bmatrix} \alpha_0 \\ \beta_0 \\ 0 \\ 0 \end{bmatrix} = c_1 \begin{bmatrix} -\sqrt{m} \\ 1 \\ 0 \\ 0 \end{bmatrix} + c_2 \begin{bmatrix} 0 \\ 0 \\ a \\ -\sqrt{m}a \end{bmatrix} + c_3 \begin{bmatrix} \sqrt{m} \\ 1 \\ 0 \\ 0 \end{bmatrix} + c_4 \begin{bmatrix} 0 \\ 0 \\ b \\ \sqrt{m}b \end{bmatrix} \tag{3.25}$$

The solution of (3.25) is,

$$c_1 = \frac{\beta_0\sqrt{m} - \alpha_0}{2\sqrt{m}},\ c_2 = 0,\ c_3 = \frac{\beta_0\sqrt{m} + \alpha_0}{2\sqrt{m}}, \text{ and } c_4 = 0$$

Hence the solution to the matrix system (3.22) is given by,

$$\mathbf{x}(t) = \frac{\beta_0\sqrt{m} - \alpha_0}{2\sqrt{m}} \begin{bmatrix} -\sqrt{m}\cos(at) \\ \cos(at) \\ -a\sin(at) \\ \sqrt{m}a\sin(at) \end{bmatrix} + \frac{\beta_0\sqrt{m} + \alpha_0}{2\sqrt{m}} \begin{bmatrix} \sqrt{m}\cos(bt) \\ \cos(bt) \\ -b\sin(bt) \\ -\sqrt{m}b\sin(bt) \end{bmatrix}$$

and we have explicit formulas for $\alpha(t)$ and $\beta(t)$; they are,

$$\alpha(t) = -\frac{\beta_0\sqrt{m} - \alpha_0}{2}\cos(at) + \frac{\beta_0\sqrt{m} + \alpha_0}{2}\cos(bt), \tag{3.26a}$$

$$\beta(t) = \frac{\beta_0\sqrt{m} - \alpha_0}{2\sqrt{m}}\cos(at) + \frac{\beta_0\sqrt{m} + \alpha_0}{2\sqrt{m}}\cos(bt). \tag{3.26b}$$

Figure 3.2 is a graph showing motion of the double pendulum governed by equations (3.26).

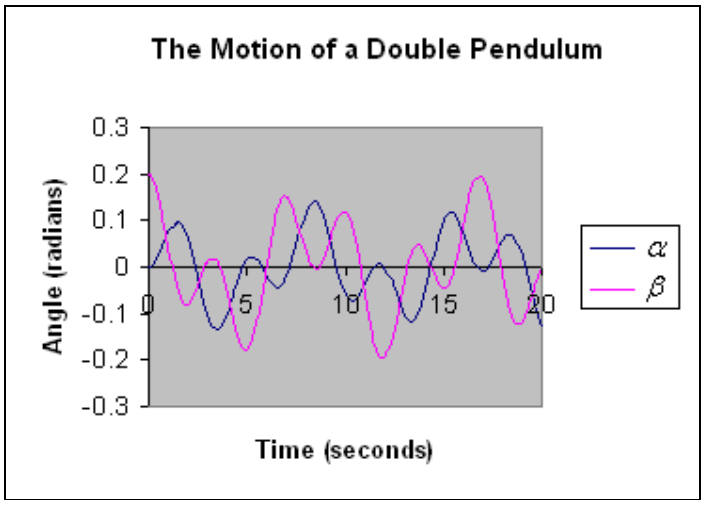


Figure 3.2 The angles of a double pendulum as time changes

To create Figure 3.2 the model was scaled, as initially for the simple pendulum, such that $c^2 = 1$, each of the bobs were given a mass of 1kg, and the initial angles for $\alpha$ and $\beta$ were $0^c$ and $0.2^c$ respectively.

I created a graph (Figure 3.3) showing the displacement on the *xy*-plane using the set of equations (3.1) for the same pendulum in Figure 3.2 to see the paths of the pendulum.

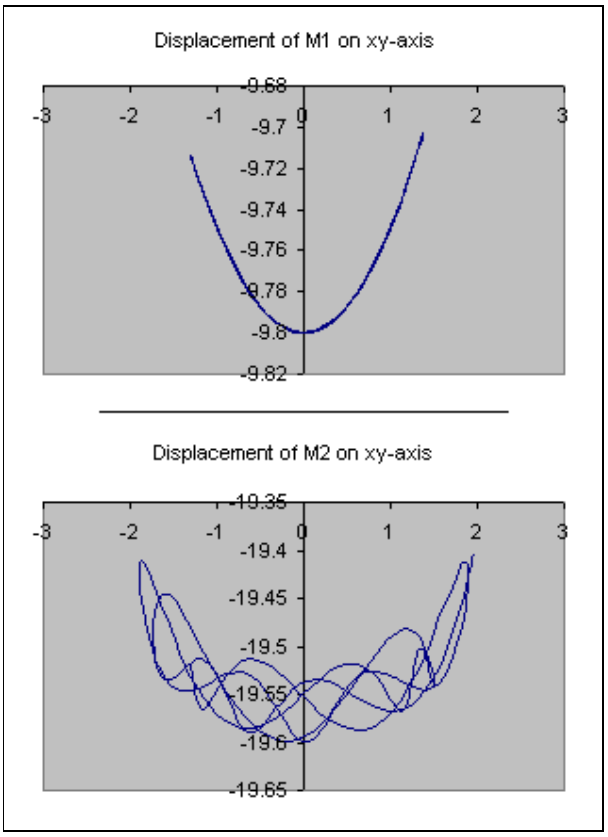


Figure 3.3 Displacement of a double pendulum, from rest for twenty seconds

From Figure 2.3 we can see that $m_1$ eventually traces out the curve of that drawn by a simple pendulum. What we cannot see, however, on this particular figure is the fact that it does not draw the arc smoothly but vibrates backwards and forwards. We can see that this is the case if we look closely at Figure 3.2 we see *extra* local minima and maxim between global minimum and maximum values. The path traced by $m_2$ is the main reason for Figure 3.3. What we cannot see from the figures is whether the motion is periodic or not. In fact, for the pendulum for Figure 3.2 the motion is *quasiperiodic*. Let us look at this motion in a bit more detail.

### 3.4 An introduction to quasiperiodic motion

Both $\alpha(t)$ and $\beta(t)$ are sums of two periodic functions. If the ratio of their frequencies is a rational number then the system shows periodic behaviour, but if the ratio is not rational then the system is *quasiperiodic*. (Jordan and Smith, 2004 page 466). This is the essence of quasiperiodic motion. I.e. if $\frac{a}{b} \notin \mathbf{Q}$ the pendulum swings with quasiperiodic motion.

If we have motion that is periodic then at some point in time the systems retraces the solution paths that it followed before. The system then continues to 'cycle' around this path with a certain frequency. If, however, the ratio of the sum of two periodic functions cannot be defined as a rational number then there is no *exact* frequency for which the motion repeats itself. Therefore as the solution path continues in time it will never retrace its own path even though it is a function described by the sum of periodic functions. The system then looks periodic but is not, this is what is meant by quasi-periodic motion.

In our example $a = \sqrt{N + N\sqrt{m}}$ and $b = \sqrt{N - N\sqrt{m}}$, hence

$$\frac{a}{b} = \frac{\sqrt{N + N\sqrt{m}}}{\sqrt{N - N\sqrt{m}}} = \left(\frac{1+\sqrt{m}}{1-\sqrt{m}}\right)^{1/2} = \left(\frac{\left(1+\sqrt{m}\right)^2}{1-m}\right)^{1/2} = \frac{1+\sqrt{m}}{\sqrt{1-m}}$$

For the double pendulum we used to create Figure 3.2 $m = \frac{1}{2}$, hence

$$\frac{a}{b} = \frac{1+\sqrt{\frac{1}{2}}}{\sqrt{1-\frac{1}{2}}} = \sqrt{2}+1$$

which is an irrational number. Hence when the bobs on a double pendulum are of equal mass the system moves with quasiperiodic motion.

Because the paths of motion do not repeat themselves in quasiperiodic motion, the curves in the phase plane never cross each other or connect together. In fact '*the solutions define an n-torus in phase space*' (Glendinning 1994, page 18). This means that the curves of the phase plane (in *n*-dimensions) appear to wrap themselves around a torus shape, whilst never crossing the pervious path. A torus shape is that of a ringed donut. It is worth noting that this torus shape does not have to be a perfect donut shape, it can be twisted and warped in the *n*-dimensions. In our case we have four dimensions ($\alpha$, $\beta$, $\lambda$ and $\mu$), and hence we expect to find that the phase paths trace out a torus in 4-dimensions. Unfortunately we cannot draw in 4-dimensions, however we can draw the phase portrait of $\alpha$ against $\mu$ to obtain a projection of this torus into 2-dimensions.

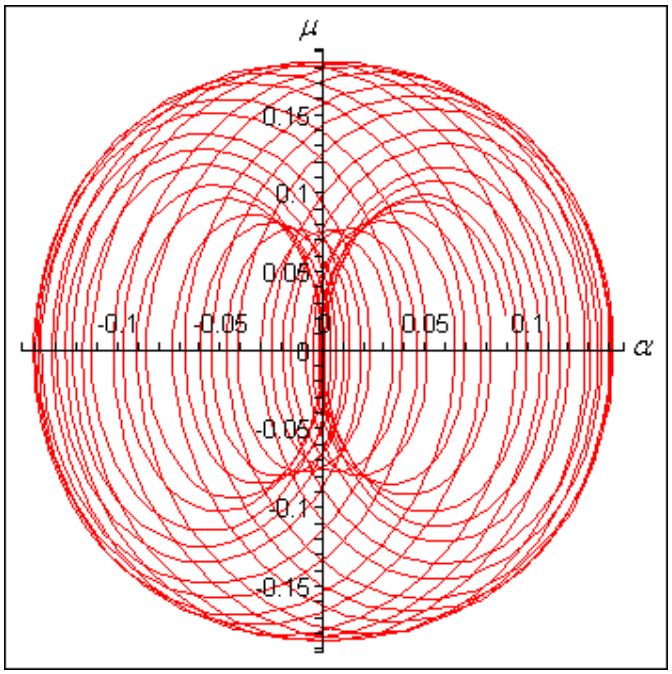


Figure 3.4. A projection of a 4-dimensional

phase portrait into 2-dimensions.

Figure 3.4 suggests the torus shape. Remember that the lines do not actually ever cross over each other in the full 4-dimensions. We can try different combinations of $\alpha$, $\beta$, $\lambda$ and $\mu$ to see different projections of the torus shape, they are all very similar to that in Figure 3.4.

We can also project this torus shape into 3-dimensions, as shown in Figure 3.5.

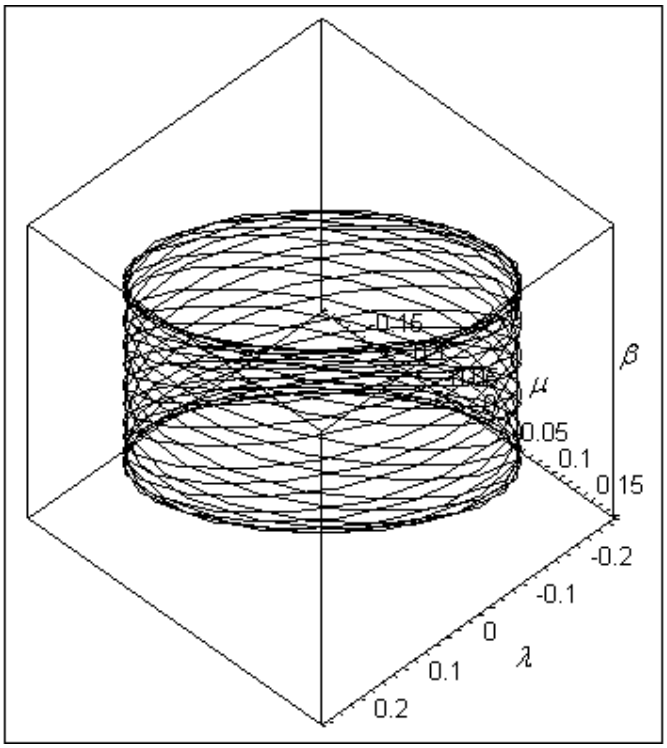


Figure 3.5. The phase path of a double pendulum project into 3-dimensions.

### 3.5 Solving the equations of motion for the double pendulum

While solving the equations of motion for small displacements is useful to obtain a sense of the way in which the double pendulum interacts, we need to remember that these results were subject to some assumptions. These assumptions may not always be valid so it also important to try and solve the equations of motion for all angles and all lengths of rods. We can do this is a similar way to solving for the earlier damped pendulum, but with more complicated formulae. We return to the equations (3.15a) and (3.15b).

$$l_1 \frac{d^2\alpha}{dt^2} + ml_2 \frac{d^2\beta}{dt^2}\cos(\beta-\alpha) - ml_2\left(\frac{d\beta}{dt}\right)^2 \sin(\beta-\alpha) + g\sin(\alpha) = 0\,, \quad (3.27a)$$

$$l_2 \frac{d^2\beta}{dt^2} + l_1 \frac{d^2\alpha}{dt^2}\cos(\beta-\alpha) + l_1\left(\frac{d\alpha}{dt}\right)^2 \sin(\beta-\alpha) + g\sin(\beta) = 0. \qquad (3.27b)$$

We need to represent the above equations as a set of first order differential equations, hence let

$$\mu = \frac{d\alpha}{dt}, \qquad (3.28a) \qquad \text{and} \qquad \lambda = \frac{d\beta}{dt}, \qquad (3.28b)$$

which leads to

$$\frac{d\mu}{dt} = \frac{d^2\alpha}{dt^2}, \qquad (3.28c) \qquad \text{and} \qquad \frac{d\lambda}{dt} = \frac{d^2\beta}{dt^2}. \qquad (3.28d)$$

Substitute (3.28) into (3.27) to give

$$l_1 \frac{d\mu}{dt} + ml_2 \frac{d\lambda}{dt}\cos(\beta-\alpha) - ml_2\lambda^2 \sin(\beta-\alpha) + g\sin(\alpha) = 0, \quad (3.29a)$$

$$l_2 \frac{d\lambda}{dt} + l_1 \frac{d\mu}{dt}\cos(\beta-\alpha) + l_1\mu^2 \sin(\beta-\alpha) + g\sin(\beta) = 0. \qquad (3.29b)$$

The equations given by (3.29) can be rearranged to give,

$$\frac{d\lambda}{dt} = \frac{g\sin(\alpha)\cos(\beta-\alpha) - l_1\mu^2 \sin(\beta-\alpha) - g\sin(\beta) - ml_2\lambda^2 \sin(\beta-\alpha)\cos(\beta-\alpha)}{l_2\left(1 - m\cos^2(\beta-\alpha)\right)}. \qquad (3.30)$$

$$\frac{d\mu}{dt} = \frac{ml_2\lambda^2 \sin(\beta-\alpha) - g\sin(\alpha) + l_1 m\mu^2 \sin(\beta-\alpha)\cos(\beta-\alpha) + gm\sin(\beta)\cos(\beta-\alpha)}{l_1\left(1 - m\cos^2(\beta-\alpha)\right)}. \qquad (3.31)$$

We now have the four first order differential equations required to solve the double pendulum – they are (3.28a), (3.28b), (3.30) and (3.31). We can implement the Runge Kutta scheme to solve this numerically, and then use the calculated $\alpha$ and $\beta$ values to draw a graph showing how the angles change with respect to time for the double pendulum

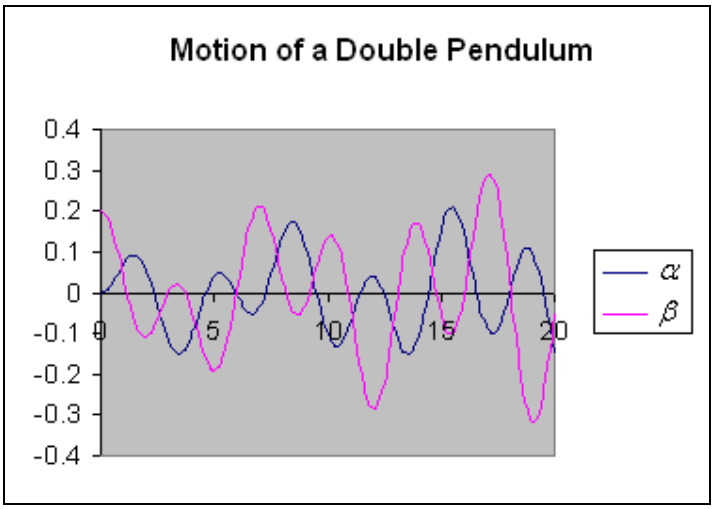


Figure 3.6. The angles of a double pendulum as time changes

Figure 3.6 is created using the same initial values as used to create the graph in Figure 3.2. We can see that the graphs look very similar but careful examination shows that they start to differ after about $t$=12. This is because the angles begin to increase and hence the assumption of small angles is no longer valid.

### 3.6 Energy in the system and coupling effects

In our system of the double pendulum we have a certain amount of energy. Einstein tells us (in his work on Relativity) that energy can be neither created nor destroyed. Because we have neglected any form of damping in our system of the double pendulum we should see that there is no loss or gain of energy. There are two types of energy in our system, *potential* and *kinetic*.

The potential energy ($V$) of the double pendulum can be found by

$$V = m_1 g y_1 + m_2 g y_2 + constant\,. \tag{3.32}$$

(The constant is there because as we raise the double pendulum further in the air, so the potential energy increases, we shall set this to zero to simplify the mathematics).

Into which we can substitute our values from (3.1b) and (3.1d) to give

$$V = -(m_1 + m_2) g l_1 \cos(\alpha) - m_2 g l_2 \cos(\beta)\,. \tag{3.33}$$

The kinetic energy ($T$) can be found by

$$T = \frac{1}{2} m_1 v_1^2 + \frac{1}{2} m_2 v_2^2\,, \tag{3.34}$$

(where relates to the speed of each bob subscripted according).

From equations (3.1)

$$v_1^2 = \left(\frac{dx_1}{dt}\right)^2 + \left(\frac{dy_1}{dt}\right)^2 = \left(l_1 \frac{d\alpha}{dt}\cos(\alpha)\right)^2 + \left(l_1 \frac{d\alpha}{dt}\sin(\alpha)\right)^2\,, \tag{3.35a}$$

$$v_2^2 = \left(\frac{dx_2}{dt}\right)^2 + \left(\frac{dy_2}{dt}\right)^2 = \left(\frac{dx_1}{dt} + l_2 \frac{d\beta}{dt}\cos(\beta)\right)^2 + \left(\frac{dy_1}{dt} + l_2 \frac{d\beta}{dt}\sin(\beta)\right)^2 . \tag{3.35b}$$

These can then be substituted into (3.34) and simplified to give

$$T = \frac{1}{2} m_1 l_1^2 \left(\frac{d\alpha}{dt}\right)^2 + \frac{1}{2} m_2 \left[ l_1^2 \left(\frac{d\alpha}{dt}\right)^2 + l_2^2 \left(\frac{d\beta}{dt}\right)^2 + 2 l_1 l_2 \frac{d\alpha}{dt}\frac{d\beta}{dt}\cos(\beta - \alpha) \right], \tag{3.36}$$

We can then use the equations to draw a graph of the total energy (i.e. $V + T$) in the system.

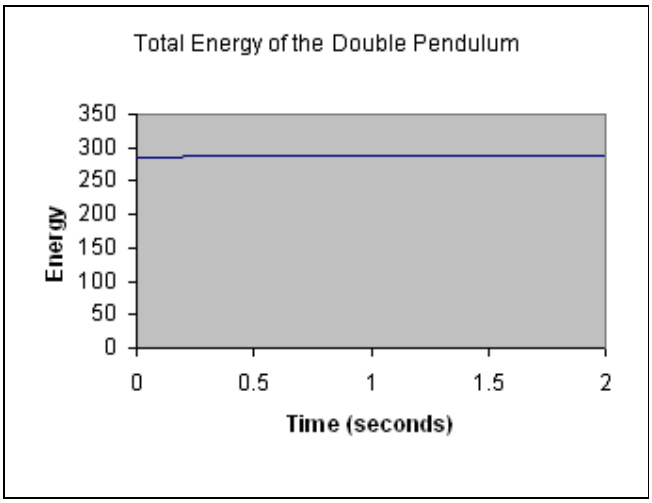


Figure 3.7. The total amount of energy in an undamped double pendulum

We can see from Figure 3.7 (the energy of the double pendulum from Figure 3.6) that the energy is approximately constant. (The actual value for energy came out negative because we stated that the constant in $V$ was zero, I have plotted the modulus purely to make the figure look better). The reason for the slight change is not due to energy entering or leaving the system, they are computational errors from our numerical iteration. This is where we remember that numerical solutions only give approximate solutions.

When there are two oscillating particles that are coupled together there can be transference of energy between them, this is known as a coupling effect. This coupling effect should be present in our double pendulum. We can look at this by examining the energy of each bob rather than the whole double pendulum.

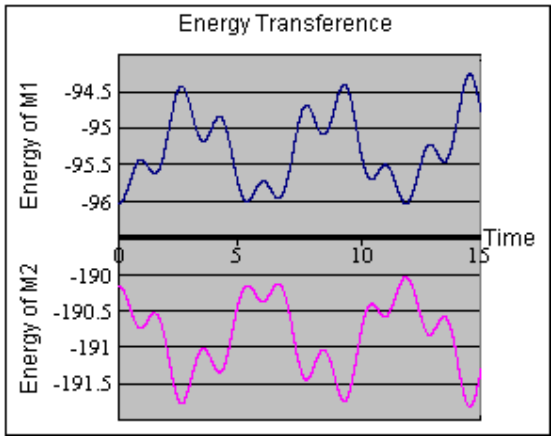


Figure 3.8. Exchange of energy between two masses of a double pendulum

Figure 3.8 shows the energy exchange for the double pendulum from Figure 3.6. Because the exchange of energy is so very small compared to the total energy it was not possible to have both the amounts of energy for each mass on the chart and still notice the transference, this is why there are not values on the chart. We can see from Figure 3.8 that the coupling effect does apply to our double pendulum; we can see that energy transfers from $m_2$ to $m_1$ and back again. This happens throughout the whole motion.

To give an idea of how small the coupling effect is in relation to the total energy of each pendulums, for the fifteen seconds Figure 3.8 represents, the difference between the lowest amount of energy for each mass and the highest amount of energy for each mass was 1.7679 Joules, compared to the average energy of $m_1$ of 95.3440 Joules and the average energy of $m_2$ of 190.9026 Joules.

# 4. Vibration of the Pivot and The Inverted Pendulum

## 4.1 The forced single pendulum

(This section is intended to simply gain an understanding of the motion, from playing with computer-generated data. Mathematical proof will follow in section 5. All the calculated results in this section are obtained by using the classical fourth order Runge Kutta scheme, with $h$=0.1).

In 1908, Andrew Stephenson, a mathematics lecturer at Manchester University, had a paper printed in the *Memoirs and Proceedings of the Manchester Literary and Philosophical Society*, Vol. 52 (8), pp. 1-10. This paper showed that it was possible to maintain a pendulum in an upright stable position by making its pivot vibrate, not left and right, but up and down.

In October 1995, David Acheson and Tom Mullin appeared on the BBC documentary programme *Tomorrow's World* demonstrating their research into extending Stephenson's idea to multiple pendulums.

Let us attempt to demonstrate this property of pendulum motion. First we return to our damped single pendulum. The equation of motion was

$$\frac{d^2\alpha}{dt^2} + k\frac{d\alpha}{dt} + c^2 \sin(\alpha) = 0. \qquad (4.1)$$

[Remember that $\alpha$ is the angle between the rod and the vertical, $k$ relates to the friction due to air resistance].

Firstly we need to reintroduce gravity and length of rod as separate quantities. Hence (4.1) becomes

$$\frac{d^2\alpha}{dt^2} + k\frac{d\alpha}{dt} + \frac{g}{l}\sin(\alpha) = 0. \tag{4.2}$$

We are going to vibrate the pivot up and down; as a result the relative gravity will change. If we let the displacement of the vibration ($q$) be shown by

$$q = a\cos(\omega t). \tag{4.3}$$

The amplitude, $a$, will be equal to how high and low the pivot moves, while $\omega$ will determine how quickly the pivot moves, this is called the drive frequency.

Gravity is an accelerating force so we will have to replace $g$ with

$$g - \frac{d^2q}{dt^2} = g + a\omega^2\cos(\omega t). \tag{4.4}$$

Therefore the equation of motion becomes

$$\frac{d^2\alpha}{dt^2} + k\frac{d\alpha}{dt} + \left(\frac{g}{l} + \frac{a\omega^2}{l}\cos(\omega t)\right)\sin(\alpha) = 0. \tag{4.5}$$

Figure 4.1 below shows a diagram of the pendulum we are now modelling.

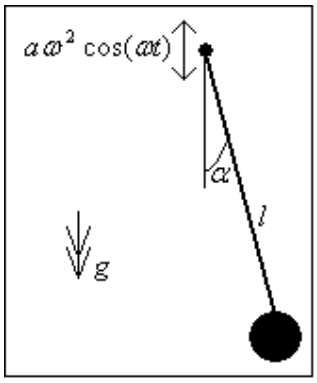


Figure 4.1. A single pendulum with a vibrating pivot.

We can solve this equation numerically as earlier, using the same numerical iteration method, except we now need to define the two new parameters $a$ and $\omega$.

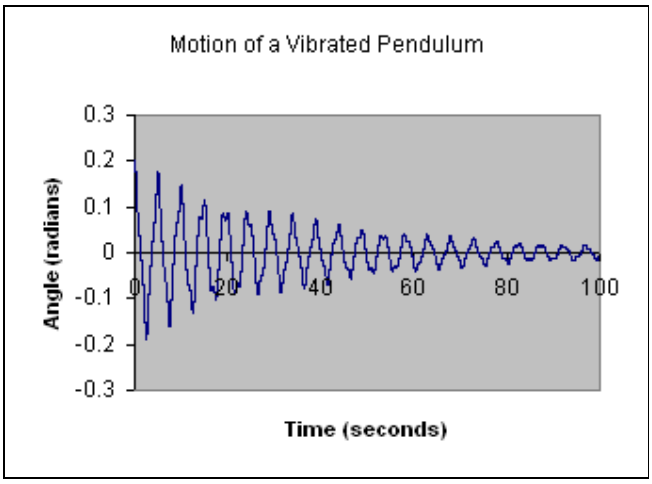


Figure 4.2. The motion of a damped pendulum with a vibrating pivot.

Figure 4.2 shows the same pendulum as we studied earlier to create Figure 2.6. $a$ and $\omega$ were given values of 2 and 5 to create the example. We can see that the vibrating motion of the pivot makes the swinging action of the pendulum 'judder' instead of flowing smoothly as we saw earlier.

Stephenson (1908) showed that the pendulum would remain in a stable inverted state if

$$\omega > \frac{\sqrt{2gl}}{a}. \qquad (4.6)$$

So for our example if we let $a$=1 then $\omega$ would have to be at least $9.8\sqrt{2}$ for the pendulum to maintain its upright position. (Note we also need to start with the pendulum in the upright position, so our initial condition is $\alpha_0 = \pi$).

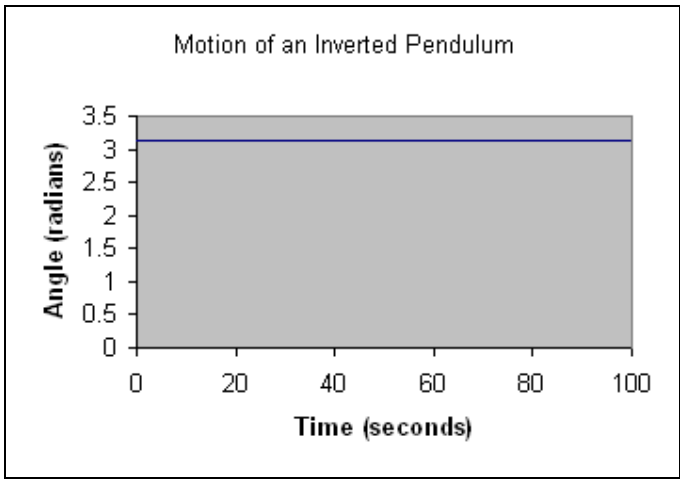


Figure 4.3. The angle between the rod of a stable inverted pendulum and the vertical

We can see from Figure 4.3 that if we apply the condition (4.6) then the pendulum is stable in the upright position, the value of $\alpha$ remains at $\pi$. The angle remains totally constant throughout the time showing that the pendulum does not deviate from the upright position, even slightly.

[It is worth noting that Acheson points out that while this all works in theory, the drive frequency needs to be a lot higher in practice. In his book *From Calculus to Chaos* (see bibliography) he notes that experiments have shown that for a pendulum with $l$=10cm and $a$=1cm, the minimum value of $\omega/2\pi$ appears to be about 22Hz, compared to the calculated minimum of 14Hz].

We can use our model to test the stability of the pendulum. Firstly, what happens if the upright pendulum is given a little push? We can represent this by changing the initial conditions and giving a value to initial speed.

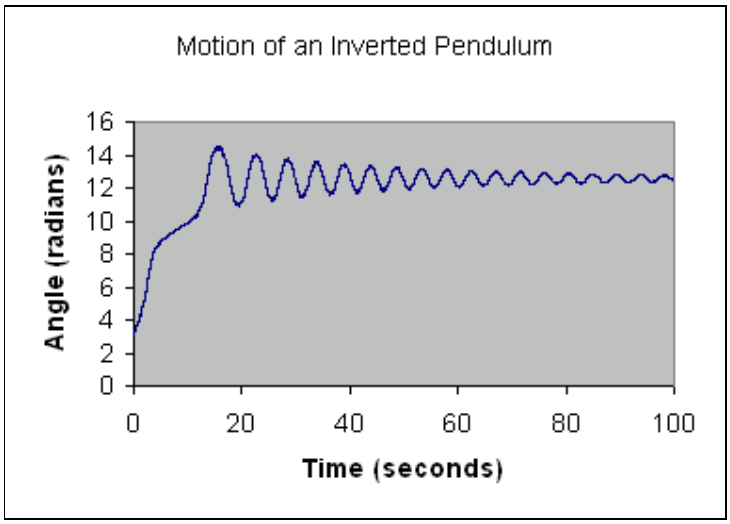


Figure 4.4. An inverted pendulum after an initial push

Figure 4.4 shows how the pendulum moves when given an initial speed of $1ms^{-1}$. We see that the pendulum spins around the pivot several times before swinging to and fro in the usual manor in the downward position. (The downward position because the angle is asymptotically converging to $4\pi$, this is two complete circles of the pivot).

It is possible to increase the frequency of the vibration and then give the pendulum a push and then, provided it did not fall into the downwards position, it does manage to maintain in the upright position.

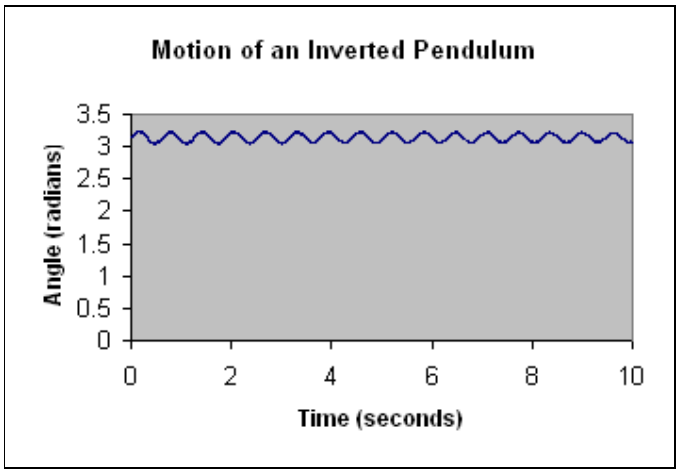


Figure 4.5. An inverted pendulum with a high frequency vibrating pivot given a push

Figure 4.5 shows a pendulum with the pivot driving frequency of nearly 200, given an initial speed of $1ms^{-1}$ (the same speed as in Figure 4.3). For a pendulum of length 10cm, vibrating at this frequency, I was able to start with an initial speed of $7.7ms^{-1}$ before the pendulum did not self-right. Another interesting point was that it is possible to take away the air resistance and the pendulum still maintains an inverted position, this means we can try the same techniques with the model of the double pendulum from section 3.

### 4.2 The forced double pendulum

The equations of motion for the double pendulum were

$$l_1 \frac{d^2\alpha}{dt^2} + ml_2 \frac{d^2\beta}{dt^2}\cos(\beta-\alpha) - ml_2\left(\frac{d\beta}{dt}\right)^2 \sin(\beta-\alpha) + g\sin(\alpha) = 0\,, \qquad (4.7a)$$

$$l_2 \frac{d^2\beta}{dt^2} + l_1 \frac{d^2\alpha}{dt^2}\cos(\beta-\alpha) + l_1\left(\frac{d\alpha}{dt}\right)^2 \sin(\beta-\alpha) + g\sin(\beta) = 0\,, \qquad (4.7b)$$

where

$$m = \frac{m_2}{m_1 + m_2}. \tag{4.7c}$$

Again we replace $g$ with (4.4) to give

$$l_1 \frac{d^2\alpha}{dt^2} + ml_2 \frac{d^2\beta}{dt^2}\cos(\beta - \alpha) - ml_2\left(\frac{d\beta}{dt}\right)^2 \sin(\beta - \alpha) + (g + a\omega^2 \cos(\omega t))\sin(\alpha) = 0, \tag{4.8a}$$

$$l_2 \frac{d^2\beta}{dt^2} + l_1 \frac{d^2\alpha}{dt^2}\cos(\beta - \alpha) + l_1\left(\frac{d\alpha}{dt}\right)^2 \sin(\beta - \alpha) + (g + a\omega^2 \cos(\omega t))\sin(\beta) = 0. \tag{4.8b}$$

We can then solve this system numerically with the minor alteration, the results of which are shown in Figure 4.6.

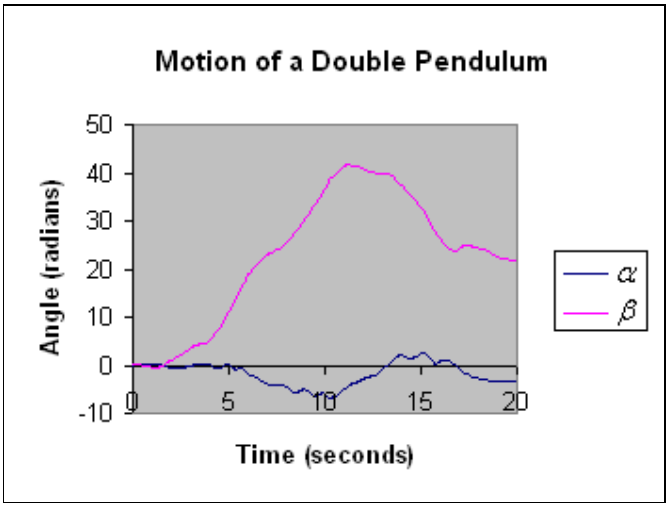


Figure 4.6 The motion of a double pendulum with a vibrated pivot.

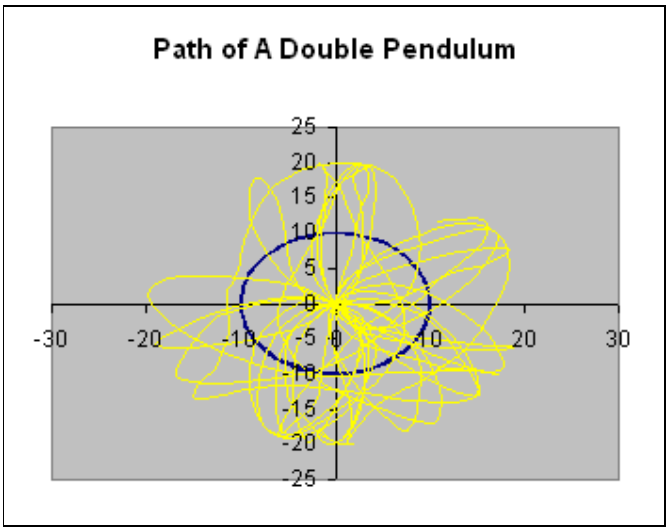


Figure 4.7. The path traced out by the double pendulum in Figure 4.6

Figures 4.6 and 4.7 show how messy the paths of the double pendulum can become. They are a typical example of a double pendulum with a vibrated pivot. The pendulum is the same used to create Figure 3.6 and $a$ and $\omega$ were set to 2 and 5 respectively.

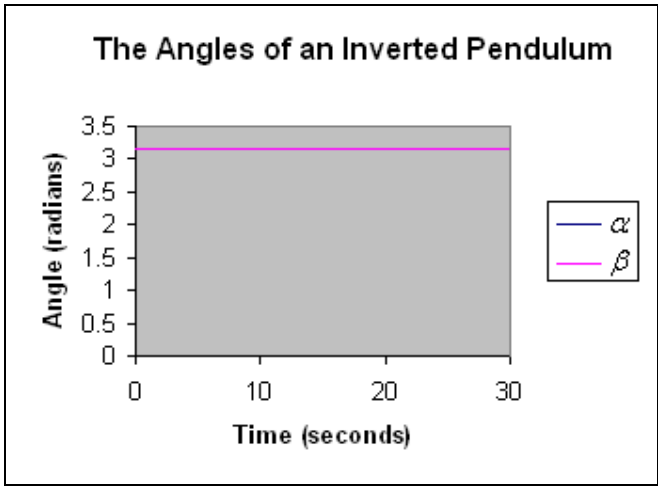


Figure 4.8 The motion of an inverted double pendulum

If we start the double pendulum in the upside-down position then, as with the single pendulum, the system can be made to remain inverted. Figure 4.8 was made using the same pendulum as Figure 4.7, except both initial angles were set at $\pi$, and $a$ and $\omega$ were given typical values of 1 and 20. It appears that $\alpha = \beta = \pi$ for all time.

Notice that the values used to invert the pendula has been rather vague. Many values were sufficient to achieve the inverted state. The only condition necessary for the single pendulum to be stabilized in the upside-down state is equation (4.6). The corresponding condition for that of $N$ pendula is (from the mentioned book by Acheson),

$$a < \frac{0.450g}{\sigma_{\max}^2}, \tag{4.9a}$$

and

$$a\omega > \frac{g\sqrt{2}}{\sigma_{\min}}. \tag{4.9b}$$

where $\sigma_{\min}$ $\sigma_{\max}$ relate to the smallest and largest *natural frequencies* (see the following section) of the system. This is interesting because this gives just two numbers needed to know about the system in order to invert it. If $N$ is large then $\sigma_{\max}$ is also usually large, hence from (4.8) $a$ would have to be very small and $\omega$ very large. In this way we see that the greater number of pendulums the more difficult it would become to achieve the inverted state practically, as one would expect.

### 4.3 Natural frequencies

The equations 4.8 naturally bring us to desiring to know about natural frequencies of systems. Figure 4.9 is taken directly from the book by Acheson (page180), it shows a typical example of how a system behaves under $\sigma_{min}$ and $\sigma_{max}$. He uses a triple pendulum to illustrate the motion more clearly.

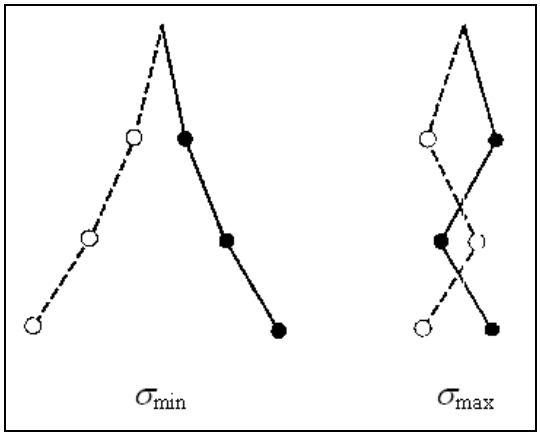


Figure 4.9 The typical motion of a downward-hanging triple pendulum corresponding to σmin and σmax.

When a system is in equilibrium, all the forces counteract each other. When the system is then moved a *restoring force* results, which tries to counteract the movement and bring the system back into equilibrium. If this restoring force is *proportional* to the displacement; when the system is released (in our case when the pendulums are allowed to swing) the frequency at which the system now moves is called its natural frequency (or characteristic frequency).

If we take equations (3.19);

$$\frac{d^2\alpha}{dt^2} + m\frac{d^2\beta}{dt^2} + \frac{g}{l}\alpha = 0, \tag{4.10a}$$

$$\frac{d^2\beta}{dt^2} + \frac{d^2\alpha}{dt^2} + \frac{g}{l}\beta = 0, \tag{4.10b}$$

we can find the natural frequencies of the system by substituting $\alpha = A\cos(\sigma t)$ and $\beta = B\cos(\sigma t)$. We find the system has two natural frequencies given by

$$\sigma^2 = \frac{g/l}{1 \pm \sqrt{m}}. \tag{4.11}$$

Similarly, if there are *N* pendulums, there are *N* natural frequencies of the system.

# 5. The Theory of the Inverted Pendulum

## 5.1 Introduction to Floquet Theory, and Hills equation

To continue in this investigation into the nature of the inverted pendulum we need to introduce *Floquet Theory*, hence in this chapter we digress slightly into this area. This is a theory that can be applied to differential equations with periodic coefficients.

Hills equation is given by,

$$u'' + a(t)u = 0\,, \tag{5.1}$$

(where $a(t)$ is any given periodic function) and is a good example for us to use in our study of Floquet theory. Recall that we modelled the motion of a pendulum with a vibrated pivot with the equation,

$$\frac{d^2\alpha}{dt^2} + k\frac{d\alpha}{dt} + \left(\frac{g}{l} + \frac{a\omega^2}{l}\cos(\omega t)\right)\sin(\alpha) = 0\,. \tag{5.2}$$

We also have shown that we can invert a pendulum governed by this equation.

The above equation is essentially Hills equation with,

$$k = 0 \quad \text{and} \quad a(t) = \frac{g}{l} + \frac{a\omega^2}{l}\cos(\omega t) \tag{5.3}$$

for small values of $\alpha$. (You may remember that if $\alpha$ is small then the pendulum is pointing downward and not inverted, this point will be looked at later).

Consider the system

$$\frac{d\mathbf{x}}{dt} = \mathbf{A}(t)\mathbf{x}, \tag{5.4a}$$

where

$$\mathbf{A}(t+T) = \mathbf{A}(t) \quad \forall t. \tag{5.4b}$$

Hence, the coefficient $\mathbf{A}(t)$ is periodic with a period $T$.

The essence of *Floquet Theory* (taken directly from Grimshaw 1990, page 47) is:

> Let $\mathbf{X}(t)$ be a fundamental matrix for (5.4a). Then $\mathbf{X}(t+T)$ is also a fundamental matrix, and there exists a non-singular constant matrix $\mathbf{B}$ such that
>
> $$\mathbf{X}(t+T) = \mathbf{X}(t)\mathbf{B} \quad \forall t. \tag{5.5}$$
>
> Also,
>
> $$\det \mathbf{B} = \exp\left\{\int_0^T \operatorname{tr} \mathbf{A}(s)\, ds\right\}. \tag{5.6}$$
>
> where det $\mathbf{B}$ is the *determinant* of matrix $\mathbf{B}$, and tr $\mathbf{A}(s)$ is the trace of the matrix (the sum of all the elements on the principle diagonal).

(For definitions and examples of *fundamental matrices*, *linearly dependent* solutions and *linearly independent* solutions see Jordan and Smith 2004, pp 292-295).

Proof of the theorem above is also given in Grimshaw (1990). However for this report we only concern ourselves with the results so we can apply them to our own problem.

Let us now look at an example of *Floquet theory* on *Hills* equation given by

$$u'' + a(t)u = 0\,, \tag{5.7a}$$

where

$$a(t+T) = a(t) \quad \forall t\,. \tag{5.7b}$$

If we let $x_1 = u$ and $x_2 = u'$ then we can express (5.7a) in the form

$$\begin{bmatrix} x_1' \\ x_2' \end{bmatrix} = \begin{bmatrix} 0 & 1 \\ -a(t) & 0 \end{bmatrix} \begin{bmatrix} x_1 \\ x_2 \end{bmatrix} \tag{5.8}$$

which is equivalent to (5.4a). Hence

$$\mathbf{A}(t) = \begin{bmatrix} 0 & 1 \\ -a(t) & 0 \end{bmatrix}. \tag{5.9}$$

We can see that

$$\text{tr}\ \mathbf{A}(t) = 0\,. \tag{5.10}$$

Also, the fundamental matrix for this particular problem is of the form

$$\mathbf{X}(t) = \begin{bmatrix} u^1(t) & u^2(t) \\ \dot{u}^1(t) & \dot{u}^2(t) \end{bmatrix} \tag{5.11}$$

where $u^1$ and $u^2$ are two linearly independent solutions of *Hills* equation.

Since (5.5) is true for all *t*, when $t = 0$,

$$\mathbf{X}(T) = \mathbf{X}(0)\mathbf{B} \tag{5.12a}$$

$$\Rightarrow\ \mathbf{B} = \mathbf{X}^{-1}(0)\mathbf{X}(T) \tag{5.12b}$$

If we start with the linear independent initial conditions

$$u^1(0) = 1,\ u^2(0) = 0,\ \dot{u}^1(0) = 0,\ \dot{u}^2(0) = 1,$$

then from (5.11),

$$\mathbf{X}(0) = \begin{bmatrix} 1 & 0 \\ 0 & 1 \end{bmatrix}. \tag{5.13}$$

Then from (5.12b),

$$B = \begin{bmatrix} u^1(T) & u^2(T) \\ \dot{u}^1(T) & \dot{u}^2(T) \end{bmatrix}. \tag{5.14}$$

Because of (5.6), (5.10) and (5.14) we can say

$$\det \begin{bmatrix} u^1(T) & u^2(T) \\ \dot{u}^1(T) & \dot{u}^2(T) \end{bmatrix} = \exp\left\{ \int_0^T 0 \, ds \right\}$$

$$\Rightarrow \quad u^1(T)\dot{u}^2(T) - u^2(T)\dot{u}^1(T) = 1. \tag{5.15}$$

Let us bring in some more definitions and results of Floquet theory. All are proven at the source given.

Definition 1: (Grimshaw 1990, page 49)

Let the eigenvalues of B (defined by Equation (5.4a)) be $\rho_1, \ldots, \rho_n$, called the **characteristic multipliers** for (5.4a). The **characteristic exponents** $\mu_1, \ldots, \mu_n$ are defined by,

$$\rho_1 = e^{\mu_1 T}, \quad \ldots, \quad \rho_n = e^{\mu_n T}.$$

Definition 2: (Grimshaw 1990, page 50)

Let $\rho$ be a (positive) characteristic multiplier for (5.4a) (in one dimension) and let $\mu$ be the corresponding characteristic exponent so that $\rho = e^{\mu T}$. Then there exists a solution $x(t)$ of (5.4a) such that,

$$x(t+T) = \rho x(t) \quad \forall t \, .$$

Further, there exists a periodic function $p(t)$ (i.e. $p(t+T)=p(t)\ \forall t$) such that,

$$x(t)=ce^{\mu t}p(t)\quad \forall t\,,$$

where $c$ is an arbitrary constant.

Similarly in $n$ dimensions,

$$x(t)=\sum_{j=1}^{n}c_j e^{\mu_j t}p_j(t)\,.$$

From Definition 1 the characteristic multipliers are given by,

$$\begin{vmatrix} u^1(T)-\rho & u^2(T) \\ \dot{u}^1(T) & \dot{u}^2(T)-\rho \end{vmatrix}=0 \tag{5.16a}$$

$$\Rightarrow\quad \left(u^1(T)-\rho\right)\left(\dot{u}^2(T)-\rho\right)-u^2(T)\dot{u}^1(T)=0 \tag{5.16b}$$

$$\Rightarrow\quad \rho^2-\rho\left(u^1(T)+\dot{u}^2(T)\right)+u^1(T)\dot{u}^2(T)-u^2(T)\dot{u}^1(T)=0 \tag{5.16c}$$

Then (5.16c) can be simplified using (5.15) to give,

$$\rho^2-\rho\left(u^1(T)+\dot{u}^2(T)\right)+1=0\,. \tag{5.17}$$

If we make the simplification,

$$u^1(T)+\dot{u}^2(T)=2\phi\,, \tag{5.18}$$

then (5.17) becomes,

$$\rho^2-2\phi\rho+1=0\,, \tag{5.19}$$

which leads to,

$$\rho_1=\phi+\sqrt{\phi^2-1}\,,\quad \rho_2=\phi-\sqrt{\phi^2-1}. \tag{5.20}$$

There are some useful relations between $\rho_1$ and $\rho_2$ that we shall use later,

$$\rho_1\rho_2=1\,,\ \rho_1+\rho_2=2\phi, \tag{5.21a}$$

and consequently,

$$\mu_1 + \mu_2 = 0\,,\ \cosh(\mu_1 T) = \phi\,, \tag{5.21b}$$

where $\mu_1$ and $\mu_2$ are the corresponding characteristic exponents of $\rho_1$ and $\rho_2$ respectively.

## 5.2 Mathieu's Equation

*Mathieu's equation* is a special form of *Hills equation* with $a(t) = \delta + \varepsilon\cos(2t)$ and is therefore given by,

$$u'' + \big(\delta + \varepsilon\cos(2t)\big)u = 0\,. \tag{5.22}$$

(Notice the similarity of Mathieu's equation and our pendulum equation, equation (5.2) with $k$=0).

Hence the Mathieu's equation can be expressed by,

$$\begin{bmatrix} x_1' \\ x_2' \end{bmatrix} = \begin{bmatrix} 0 & 1 \\ -\delta - \varepsilon\cos(2t) & 0 \end{bmatrix}\begin{bmatrix} x_1 \\ x_2 \end{bmatrix}, \tag{5.23}$$

as a first order system. From the last section we discovered that the characteristic multipliers for this system are given by (5.20). By Definition 1, the characteristic exponents ( $\mu_1$ and $\mu_2$ ) are given by,

$$\rho_1 = e^{\mu_1 T}\,, \quad \rho_2 = e^{\mu_2 T}\,. \tag{5.24}$$

The purpose of using Floquet Theory on Mathieu's equation is to explain the stability of the solution in terms of $\delta$, and $\varepsilon$. This is where this theory links into the inverted pendulum, but more on that later. For now we concentrate on finding the stability of solutions to Mathieu's equation.

Because the solution of Mathieu's equation is dependent on $\rho_1$ and $\rho_2$ we can see from (5.20) that we have five cases to consider, namely when $\phi < -1$, $\phi = -1$, $-1 < \phi < 1$, $\phi = 1$, and $\phi > 1$. This is because these are the values when solutions vary between real and complex solutions and repeated solutions of (5.20).

Let us consider each case separately;

**(i)** $\phi < -1$: In this instance $\rho_1$ and $\rho_2$ are both real and negative. It can be shown that $\rho_2 < -1 < \rho_1 < 0$. In this instance, because we cannot take the natural logarithm of a negative number, Definition 1 is modified slightly (see Grimshaw 1990, page 52 for proof) such that

$$\mu_1 = \frac{i\pi}{T} - \nu_1 , \text{ where, } e^{\nu_1 T} = -\rho_1 .$$

Thus $v$ is a real function and we can use Definition 2. Because of this modification $p(t)$ in Definition 2 becomes $q(t)$ where,

$$q(t) = \exp\left(\frac{i\pi t}{T}\right) p(t)$$

and $q(t)$ is periodic with a period of $2T$ (again see Grimshaw page 52 for details). Also note that as a consequence of (5.21b), $\mu_2 = -\mu_1$. Hence the solution is given by

$$u(t) = c_1 e^{-\nu_1 t} q_1(t) + c_2 e^{\nu_1 t} q_2(t) , \qquad (5.25a)$$

where,

$$q_{1,2}(t + 2T) = q_{1,2}(t) \quad \forall t . \qquad (5.25b)$$

Therefore solution when $\phi < -1$ is, in general, $|u(t)| \to \infty$ as $t \to \infty$, and hence (5.25a) describe *unstable* behaviour.

**(ii)** $\phi = -1$: In this case we have just one real characteristic multiplier, i.e. $\rho_1 = \rho_2 = \rho$. Hence we only have one characteristic exponent. Again because $\rho$ is negative ( $\rho = -1$) so we need to use our modified form of Definition 1 as we did in **(i)**. This case can be regarded as the limit $v_1 \to 0$ (see Grimshaw, page 60), and the general solution is given by,

$$u(t) = c_1 q_1(t) + c_2 \{ktq_1(t) + q_2(t)\}, \tag{5.26a}$$

where,

$$q_{1,2}(t + 2T) = q_{1,2}(t) \quad \forall t, \tag{5.26b}$$

and $k$ is an arbitrary constant. For this case, because of (5.26a) the solution is bounded for certain values of $c_2$ and $k$ and therefore we have *marginal stability*. Notice that when $c_2$=0 we have a solution with a fundamental period of $2T$.

**(iii)** $-1 < \phi < 1$: For this case $\rho_1$ and $\rho_2$ are both complex. Details of how we deal with complex values are set out on page 52 of Grimshaw 1990. The results of this are that,

$$\rho_{1,2} = \exp(\pm i\sigma T), \ \mu_1 = i\sigma,$$

where

$$\cos(\sigma T) = \phi \quad (0 < \sigma T < \pi).$$

And the general solution is given by,

$$u(t) = c_1 \,\mathrm{Re}\left\{e^{i\sigma t}\, p(t)\right\} + c_2 \,\mathrm{Im}\left\{e^{i\sigma t}\, p(t)\right\}, \tag{5.27a}$$

where,

$$p(t+T) = p(t) \quad \forall t\,. \tag{5.27b}$$

Here, although $p(t)$ is complex it is also periodic (this time with a fundamental period of $T$). The solution is again bounded, oscillatory and *stable*.

**(iv)** $\phi = 1$: Now we have one real characteristic multiplier. This case is the same as in **(ii)**, except now we do not need to introduce the $q(t)$ modification because $\rho = 1$, and is therefore positive. Hence the general solution to (5.22) is given by,

$$u(t) = c_1 p_1(t) + c_2 \left\{k t p_1(t) + p_2(t)\right\}, \tag{5.28a}$$

where,

$$p_{1,2}(t+T) = p_{1,2}(t) \quad \forall t\,, \tag{5.28b}$$

This case can be seen as when $\mu_1 \to 0$ because ( $\rho = e^{\mu T}$ ) in **(v)**. Again we have a case of *marginal stability*. Notice that when $c_2 = 0$ the solution (5.28a) is periodic with a fundamental period of $T$.

**(v)** $\phi > 1$: This is the simplest case because both $\rho_1$ and $\rho_2$ are real and positive, and we can use Definitions 1 and 2 in their explicit form. Notice that $\rho_1 > 1 > \rho_2 > 0$. Consequently $\mu_1$ is real and positive and from (5.21b), $\mu_2 = -\mu_1$. Hence from Definition 2,

$$u(t) = c_1 e^{\mu_1 t}\, p_1(t) + c_2 e^{-\mu_1 t}\, p_2(t)\,, \tag{5.29a}$$

where,

$$p_{1,2}(t+T) = p_{1,2}(t) \quad \forall t\,. \tag{5.29b}$$

If we look at (5.29a) we can see that $u(t) \to \infty$ as $t \to \infty$ and the solution is unstable.

The interesting result from this analysis is the boundaries between stable and unstable solutions of (5.22). These boundaries are given by the boundaries $\phi = \pm 1$. We have seen that when $\phi = 1$ we can have periodic solutions with a fundamental period of *T*, and when $\phi = -1$ we can have solutions with a fundamental period of 2*T*. The idea now is to draw curves of these boundaries in the $\delta$-$\varepsilon$ plane so we will know if the solutions to the Mathieu equation are stable or unstable for any given values of $\delta$ and $\varepsilon$. We shall refer to the curves in the $\delta$-$\varepsilon$ plane as the *stability boundaries*.

### 5.3 The Stability Boundaries of Mathieu's Equation (Fourier Series)

Let us first look at the case when $\varepsilon = 0$. In this case (5.22) becomes,

$$u'' + \delta u = 0\,.$$

The above equation has the solution,

$$u = c_1 \cos\left(\sqrt{\delta}t\right) + c_2 \sin\left(\sqrt{\delta}t\right),$$

and is periodic with a fundamental period of $T = 2\pi/\sqrt{\delta}$. From (5.13) we find that,

$$u^1 = \cos\left(\sqrt{\delta}t\right) \qquad \text{and} \qquad u^2 = \frac{1}{\sqrt{\delta}}\sin\left(\sqrt{\delta}t\right).$$

From (5.18) we can see that,

$$\phi = \cos\left(\sqrt{\delta}T\right). \tag{5.30}$$

Recall that we are interested in the stability boundaries, and these occur at $\phi = \pm 1$. When $\phi = 1$ we can see from (5.30) that $\sqrt{\delta}T = 2k\pi$, and when $\phi = -1$ we can see that $\sqrt{\delta}T = (2k+1)\pi$. (Where $k = 0, 1, 2, \ldots$). Hence we know that the stability boundaries will pass through the $\varepsilon$-axis at these points, and as such if there are small regions of instability for $|\varepsilon|$ they must be centred on these points. As we mentioned in our case $T = \pi$, so the points on the $\varepsilon$-axis will be given by,

$$\sqrt{\delta} = 2k \qquad \text{and} \qquad \sqrt{\delta} = 2k+1$$

or alternatively,

$$\delta = (2k)^2 \qquad \text{and} \qquad \delta = (2k+1)^2. \tag{5.31}$$

Now let us consider when $\varepsilon \neq 0$. At the end of section 5.2 we found that the stability boundaries were given by solutions that were periodic, with periods $T$ and $2T$. We could try to find these solutions in terms of a *Fourier series* (see Mathematical Techniques, Jordan and Smith for details on *Fourier Series*) for $u(t)$. We will be looking for a solution to equation (5.22) of the form,

$$u(t) = \tfrac{1}{2}a_0 + \sum_{n=1}^{\infty}\left(a_n \cos(nt) + b_n \sin(nt)\right). \tag{5.32}$$

We can use a Fourier series for $u$ with a period of $2\pi$ to obtain solutions for $\pi$ by setting to zero the Fourier coefficients when $n$ is and odd number. We wish to do this because we can see from (5.22) that $T = \pi$ in our case, and from the analysis at the

end of section 5.2 we found the stability boundaries are defined by solutions of fundamental period $T$ and $2T$.

From (5.32) we find that,

$$u''(t) = \sum_{n=1}^{\infty} -n^2 a_n \cos(nt) - n^2 b_n \sin(nt). \tag{5.33}$$

Also, if we multiply (5.32) by $\cos(2t)$ we obtain,

$$\cos(2t)u(t) = \tfrac{1}{2} a_0 \cos(2t) + \sum_{n=1}^{\infty} \left( a_n \cos(2t)\cos(nt) + b_n \cos(2t)\sin(nt) \right). \tag{5.34}$$

Substituting the trigonometric identities,

$$2\cos(2t)\cos(nt) = \cos\left((n+2)t\right) + \cos\left((n-2)t\right), \tag{5.35a}$$

$$2\cos(2t)\sin(nt) = \sin\left((n+2)t\right) + \sin\left((n-2)t\right), \tag{5.35b}$$

into (5.34) we get,

$$\begin{aligned}\cos(2t)u(t) = \tfrac{1}{2} a_0 \cos(2t) &+ \tfrac{1}{2} \sum_{n=1}^{\infty} a_n \left[\cos\left((n+2)t\right) + \cos\left((n-2)t\right)\right] \\ &+ \tfrac{1}{2} \sum_{n=1}^{\infty} b_n \left[\sin\left((n+2)t\right) + \sin\left((n-2)t\right)\right]\end{aligned} \tag{5.36}$$

We note the following equalities,

$$\sum_{n=1}^{\infty} a_n \cos\left((n+2)t\right) = \sum_{n=3}^{\infty} a_{n-2} \cos(nt), \tag{5.37a}$$

$$\begin{aligned}\sum_{n=1}^{\infty} a_n \cos\left((n-2)t\right) &= a_1 \cos(-t) + a_2 \cos(0) + \sum_{n=3}^{\infty} a_n \cos\left((n-2)t\right) \\ &= a_1 \cos(t) + a_2 + \sum_{n=1}^{\infty} a_{n+2} \cos(nt),\end{aligned} \tag{5.37b}$$

$$\sum_{n=1}^{\infty} b_n \sin\left((n+2)t\right) = \sum_{n=3}^{\infty} b_{n-2} \sin(nt), \tag{5.37c}$$

$$\sum_{n=1}^{\infty} b_n \sin\big((n-2)t\big) = b_1 \sin(-t) + b_2 \sin(0) + \sum_{n=3}^{\infty} b_n \sin\big((n-2)t\big)$$

$$= -b_1 \sin(t) + \sum_{n=1}^{\infty} b_{n+2} \sin(nt)\,. \tag{5.37d}$$

Substitute equations (5.37) into (5.36) to give,

$$\begin{aligned}\cos(2t)u(t) = {} & \tfrac{1}{2} a_0 \cos(2t) + \tfrac{1}{2} \sum_{n=3}^{\infty} a_{n-2} \cos(nt) \\ & + \tfrac{1}{2} \left[ \sum_{n=1}^{\infty} a_{n+2} \cos(nt) + a_1 \cos(t) + a_2 \right] \\ & + \tfrac{1}{2} \sum_{n=3}^{\infty} b_{n-2} \sin(nt) \\ & + \tfrac{1}{2} \left[ \sum_{n=1}^{\infty} b_{n+2} \sin(nt) - b_1 \sin(t) \right]\end{aligned} \tag{5.38}$$

We can then substitute (5.38) and (5.33) and (5.32) into (5.22) to give,

$$\begin{aligned}& \sum_{n=1}^{\infty} -n^2 a_n \cos(nt) - n^2 b_n \sin(nt) \\ & + \delta\left( \tfrac{1}{2} a_0 + \sum_{n=1}^{\infty} \big( a_n \cos(nt) + b_n \sin(nt) \big) \right) \\ & + \frac{\varepsilon}{2} \left( \begin{array}{l} a_0 \cos(2t) + \sum_{n=3}^{\infty} a_{n-2} \cos(nt) \\ + \sum_{n=1}^{\infty} a_{n+2} \cos(nt) + a_1 \cos(t) + a_2 \\ + \sum_{n=3}^{\infty} b_{n-2} \sin(nt) \\ + \sum_{n=1}^{\infty} b_{n+2} \sin(nt) - b_1 \sin(t) \end{array} \right) = 0\end{aligned} \tag{5.39}$$

Since (5.39) is true for all $t$, and the stable solutions found require $u(t) \to 0$ as $t \to \infty$, the coefficients of each term must be equal to zero.

**Equating coefficients**

| | |
|---|---|
| Constant terms: | $\frac{1}{2}\delta a_0 + \frac{1}{2}\varepsilon a_2 = 0$ |
| $\cos(t)$ : | $(\delta - 1)a_1 + \frac{1}{2}\varepsilon(a_1 + a_3) = 0$ |
| $\cos(2t)$ : | $(\delta - 2^2)a_2 + \frac{1}{2}\varepsilon(a_0 + a_4) = 0$ |
| $\cos(3t)$ : | $(\delta - 9^2)a_3 + \frac{1}{2}\varepsilon(a_1 + a_5) = 0$ |
| $\vdots$ | $\vdots$ |
| $\cos(nt)$ : | $(\delta - n^2)a_n + \frac{1}{2}\varepsilon(a_{n-2} + a_{n+2}) = 0$ |
| $\sin(t)$ : | $(\delta - 1)b_1 + \frac{1}{2}\varepsilon(b_3 - b_1) = 0$ |
| $\sin(2t)$ : | $(\delta - 4)b_2 + \frac{1}{2}\varepsilon b_4 = 0$ |
| $\sin(3t)$ : | $(\delta - 9)b_3 + \frac{1}{2}\varepsilon(b_1 + b_5) = 0$ |
| $\vdots$ | $\vdots$ |
| $\sin(nt)$ : | $(\delta - n^2)b_n + \frac{1}{2}\varepsilon(b_{n-2} + b_{n+2}) = 0$ |

It can be seen that equating the coefficients results in four different sequences. These are for $a_1, a_3, a_5, \ldots, a_{2m+1}$ and $a_0, a_2, a_4, \ldots, a_{2m}$ from the cos(*nt*) terms, and $b_1, b_3, b_5, \ldots, b_{2m+1}$ and $b_2, b_4, \ldots, b_{2m}$ from the sin(*nt*) terms. As we stated before, the even subscripts relate to solutions of (5.39) with a fundamental period of $\pi$, and the odd subscripts relate to solutions with a fundamental period of $2\pi$. These are then the boundaries of $\phi = 1$ and $\phi = -1$ respectively.

If we take the coefficients of cos(*nt*) then we can see that,

$$\begin{aligned} & (\delta - n^2)a_n + \tfrac{1}{2}\varepsilon(a_{n-2} + a_{n+2}) = 0 \\ \Rightarrow \quad & \varepsilon\{2(\delta - n^2)\}^{-1} a_{n-2} + a_n + \varepsilon\{2(\delta - n^2)\}^{-1} a_{n-2} = 0 \end{aligned} \qquad (5.40)$$

If we make the simplification,

$$V_r = \varepsilon\left\{2\left(\delta - r^2\right)\right\}^{-1}.$$

Then (5.40) becomes,

$$V_n a_{n-2} + a_n + V_n a_{n+2} = 0. \tag{5.41}$$

[Note that $V_0 = \varepsilon\delta^{-1}$ is the exception in our simplification].

It is possible to set up the coefficient series in a matrix from using the simplification (5.41). The matrix for the $a_0, a_2, a_4, \ldots, a_{2m}$ series is,

$$\begin{bmatrix} 1 & V_0 & 0 & 0 & \cdots & 0 & 0 & 0 \\ V_2 & 1 & V_2 & 0 & \cdots & 0 & 0 & 0 \\ 0 & V_4 & 1 & V_4 & \cdots & 0 & 0 & 0 \\ 0 & 0 & V_6 & 1 & \cdots & 0 & 0 & 0 \\ \vdots & \vdots & \vdots & \vdots & \ddots & \vdots & \vdots & \vdots \\ 0 & 0 & 0 & 0 & \cdots & 1 & V_{n-4} & 1 \\ 0 & 0 & 0 & 0 & \cdots & V_{n-2} & 1 & V_{n-2} \\ 0 & 0 & 0 & 0 & \cdots & 0 & V_n & 1 \end{bmatrix} \begin{bmatrix} a_0 \\ a_2 \\ \vdots \\ \vdots \\ \vdots \\ \vdots \\ \vdots \\ a_n \end{bmatrix} = \begin{bmatrix} 0 \\ 0 \\ \vdots \\ \vdots \\ \vdots \\ \vdots \\ \vdots \\ 0 \end{bmatrix} \tag{5.42}$$

In (5.42) $n = 2m$ and is an even integer.

The $b_2, b_4, \ldots, b_{2m}$ sequence matrix system becomes,

$$\begin{bmatrix} 1 & V_2 & 0 & \cdots & 0 & 0 & 0 \\ V_4 & 1 & V_4 & \cdots & 0 & 0 & 0 \\ 0 & V_6 & 1 & \cdots & 0 & 0 & 0 \\ \vdots & \vdots & \vdots & \ddots & \vdots & \vdots & \vdots \\ 0 & 0 & 0 & \cdots & 1 & V_{n-4} & 1 \\ 0 & 0 & 0 & \cdots & V_{n-2} & 1 & V_{n-2} \\ 0 & 0 & 0 & \cdots & 0 & V_n & 1 \end{bmatrix} \begin{bmatrix} b_2 \\ b_4 \\ \vdots \\ \vdots \\ \vdots \\ \vdots \\ b_n \end{bmatrix} = \begin{bmatrix} 0 \\ 0 \\ \vdots \\ \vdots \\ \vdots \\ \vdots \\ 0 \end{bmatrix} \tag{5.43}$$

again $n = 2m$ and is an even integer.

The $a_1, a_3, a_5, \ldots, a_{2m+1}$ sequence matrix system becomes,

$$\begin{bmatrix} 1+V_1 & V_1 & 0 & 0 & \cdots & 0 & 0 & 0 \\ V_3 & 1 & V_3 & 0 & \cdots & 0 & 0 & 0 \\ 0 & V_5 & 1 & V_5 & \cdots & 0 & 0 & 0 \\ 0 & 0 & V_7 & 1 & \cdots & 0 & 0 & 0 \\ \vdots & \vdots & \vdots & \vdots & \ddots & \vdots & \vdots & \vdots \\ 0 & 0 & 0 & 0 & \cdots & 1 & V_{n-4} & 1 \\ 0 & 0 & 0 & 0 & \cdots & V_{n-2} & 1 & V_{n-2} \\ 0 & 0 & 0 & 0 & \cdots & 0 & V_n & 1 \end{bmatrix} \begin{bmatrix} a_1 \\ a_3 \\ \vdots \\ \vdots \\ \vdots \\ \vdots \\ \vdots \\ a_n \end{bmatrix} = \begin{bmatrix} 0 \\ 0 \\ \vdots \\ \vdots \\ \vdots \\ \vdots \\ \vdots \\ 0 \end{bmatrix} \tag{5.44}$$

here $n = 2m+1$ and is an odd integer.

The $b_1, b_3, b_5, \ldots, b_{2m+1}$ sequence matrix system becomes,

$$\begin{bmatrix} 1-V_1 & V_1 & 0 & 0 & \cdots & 0 & 0 & 0 \\ V_3 & 1 & V_3 & 0 & \cdots & 0 & 0 & 0 \\ 0 & V_5 & 1 & V_5 & \cdots & 0 & 0 & 0 \\ 0 & 0 & V_7 & 1 & \cdots & 0 & 0 & 0 \\ \vdots & \vdots & \vdots & \vdots & \ddots & \vdots & \vdots & \vdots \\ 0 & 0 & 0 & 0 & \cdots & 1 & V_{n-4} & 1 \\ 0 & 0 & 0 & 0 & \cdots & V_{n-2} & 1 & V_{n-2} \\ 0 & 0 & 0 & 0 & \cdots & 0 & V_n & 1 \end{bmatrix} \begin{bmatrix} b_1 \\ b_3 \\ \vdots \\ \vdots \\ \vdots \\ \vdots \\ \vdots \\ b_n \end{bmatrix} = \begin{bmatrix} 0 \\ 0 \\ \vdots \\ \vdots \\ \vdots \\ \vdots \\ \vdots \\ 0 \end{bmatrix} \tag{5.45}$$

again $n = 2m+1$ and is an odd integer.

The above matrix equations either admit the trivial solution or the determinant of the coefficient matrix is equal to zero. Hence there is a relations ship between $\delta$ and $\varepsilon$ for which coefficient matrix is zero.

A Fourier series converges to the exact solution of a problem as $n \to \infty$. Hence we can truncate the matrix system at a sufficiently high value of *n* (we shall define how far a little later on) and then numerically evaluate the finite determinants of the coefficient matrices. This will give us a function (of $V_r$, and hence $\delta$ and $\varepsilon$) of the

coefficients of the Fourier series that we can then plot on the $\delta\varepsilon$-plane. Recall that the curves in this plane will essentially be when $\phi = \pm 1$ from the end of Section 5.2, and hence are the boundaries between stable and unstable solutions for the Mathieu equation.

Let us begin by considering the coefficient matrix from (5.52) (for the $a_0, a_2, a_4, \ldots, a_{2m}$ sequence).

$$D_n = \det\begin{bmatrix} 1 & V_0 & 0 & 0 & \cdots & 0 & 0 & 0 \\ V_2 & 1 & V_2 & 0 & \cdots & 0 & 0 & 0 \\ 0 & V_4 & 1 & V_4 & \cdots & 0 & 0 & 0 \\ 0 & 0 & V_6 & 1 & \cdots & 0 & 0 & 0 \\ \vdots & \vdots & \vdots & \vdots & \ddots & \vdots & \vdots & \vdots \\ 0 & 0 & 0 & 0 & \cdots & 1 & V_{n-4} & 1 \\ 0 & 0 & 0 & 0 & \cdots & V_{n-2} & 1 & V_{n-2} \\ 0 & 0 & 0 & 0 & \cdots & 0 & V_n & 1 \end{bmatrix} \tag{5.46}$$

From (5.46) $D_0 = 1$ and $D_2 = 1 - V_0 V_2$, these can be calculated using standard formula.

If we use the bottom row of $D_4$ then,

$$\begin{aligned} D_4 &= \begin{vmatrix} 1 & V_0 & 0 \\ V_2 & 1 & V_2 \\ 0 & V_4 & 1 \end{vmatrix} = 0\begin{vmatrix} V_0 & 0 \\ 1 & V_2 \end{vmatrix} - V_4\begin{vmatrix} 1 & 0 \\ V_2 & V_2 \end{vmatrix} + 1\begin{vmatrix} 1 & V_0 \\ V_2 & 1 \end{vmatrix} \\ &= D_2 - V_4\begin{vmatrix} 1 & 0 \\ V_2 & V_2 \end{vmatrix} = D_2 - V_4 V_2. \end{aligned}$$

Next let us compute $D_6$, again using the last row,

$$
\begin{aligned}
D_6 &= \begin{vmatrix} 1 & V_0 & 0 & 0 \\ V_2 & 1 & V_2 & 0 \\ 0 & V_4 & 1 & V_4 \\ 0 & 0 & V_6 & 1 \end{vmatrix} \\
&= -0\begin{vmatrix} V_0 & 0 & 0 \\ 1 & V_2 & 0 \\ V_4 & 1 & V_4 \end{vmatrix} + 0\begin{vmatrix} 1 & 0 & 0 \\ V_2 & V_2 & 0 \\ 0 & 1 & V_4 \end{vmatrix} - V_6\begin{vmatrix} 1 & V_0 & 0 \\ V_2 & 1 & 0 \\ 0 & V_4 & V_4 \end{vmatrix} + 1\begin{vmatrix} 1 & V_0 & 0 \\ V_2 & 1 & V_2 \\ 0 & V_4 & 1 \end{vmatrix} \\
&= D_4 - V_6\left\{0\begin{vmatrix} V_2 & 1 \\ 0 & V_4 \end{vmatrix} - 0\begin{vmatrix} 1 & V_0 \\ 0 & V_4 \end{vmatrix} + V_4\begin{vmatrix} 1 & V_0 \\ V_2 & 1 \end{vmatrix}\right\} \\
&= D_4 - V_6V_4D_2
\end{aligned}
$$

If we continue in this manor we find that we can calculate the determinants using the following recurrence relation,

$$D_n = D_{n-2} - V_nV_{n-2}D_{n-4}\,. \tag{5.47}$$

using the initial values of,

$$D_0 = 1 \text{ and } D_2 = 1 - V_0V_2\,.$$

(recall that *n* is an even integer).

For the coefficient matrix in (5.43) relating to the $b_2, b_4, \ldots, b_{2m}$ sequence, we can see the obvious similarity to that of the coefficient matrix in (5.42) (it is the same matrix with the first row and first column removed). The recurrence relation is again (5.47), but this time it is easy to see that the initial values are given by,

$$D_2 = 1 \text{ and } D_4 = 1 - V_2V_4\,,$$

and again *n* is and even integer.

The recurrence relations for both the coefficient matrix in (5.44) and in (5.45) is again given by (5.47). The initial values for the $a_1, a_3, a_5, \ldots, a_{2m+1}$ sequence are given by,

$$D_1 = 1 + V_1 \text{ and } D_3 = 1 + V_1 - V_1 V_3.$$

The initial values for the $b_1, b_3, b_5, \ldots, b_{2m+1}$ sequence are given by,

$$D_1 = 1 - V_1 \text{ and } D_3 = 1 - V_1 - V_1 V_3.$$

Recall that,

$$V_r = \varepsilon \left\{ 2\left(\delta - r^2\right) \right\}^{-1}.$$

If we then use the above substitution and the recurrence relation (and initial values) for the $a_0, a_2, a_4, \ldots, a_{2m}$ sequence we find that,

$$\begin{aligned}
&D_0 = 1, \\
&D_2 = 1 - \varepsilon \{2\delta\}^{-1} \varepsilon \left\{ 2\left(\delta - 2^2\right) \right\}^{-1} \\
&D_4 = 1 - \varepsilon \{2\delta\}^{-1} \varepsilon \left\{ 2\left(\delta - 2^2\right) \right\}^{-1} - \varepsilon \left\{ 2\left(\delta - 4^2\right) \right\}^{-1} \varepsilon \left\{ 2\left(\delta - 2^2\right) \right\}^{-1} \cdot 1 \\
&\text{etc.}
\end{aligned}$$

Each of these determinants need to be equated to zero, and hence (for each determinant) we have a function involving only $\delta$ and $\varepsilon$. (Remember that the curves that this function plots out in the $\delta\varepsilon$-plane are boundaries between the stable and unstable solutions of the Mathieu equation). The question now is to determine how far wee need to go in the series. Figure 5.1 shows some of these curves plotted using Maple.

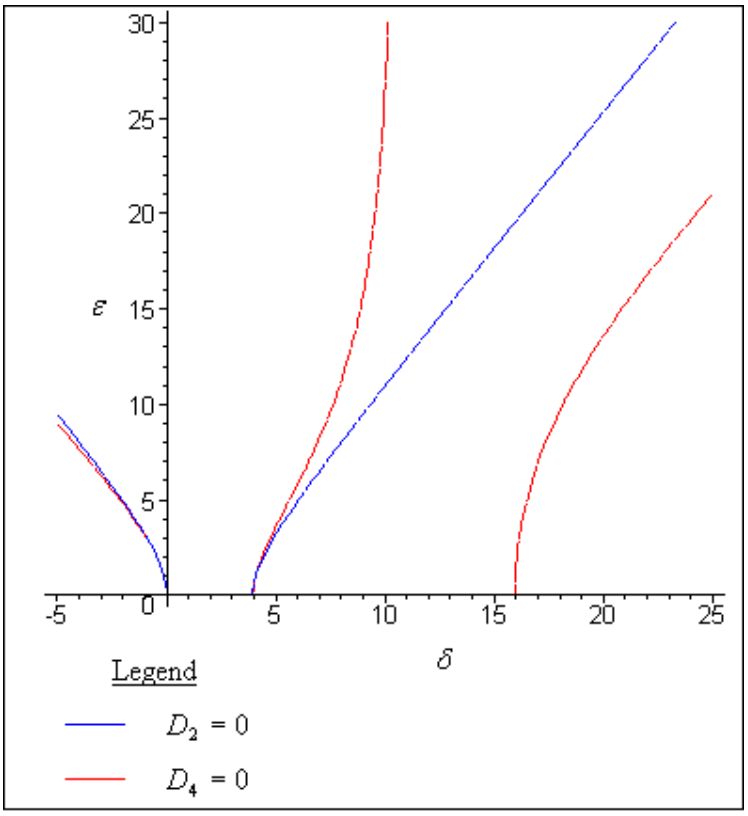


Figure 5.1 Curves in the $\delta\varepsilon$-plane defined by $D_2$ and $D_4$.

We know that the curves produced by $D_4$=0 are more accurate than $D_2$=0, so when these curves begin to split apart (notice they are almost identically when $\varepsilon$ is small) we know it is sensible to follow the $D_4$ curve rather than the $D_2$ curve. We can then plot the curves defined by $D_6$=0, and when these split apart from those defined by $D_4$=0 we follow the $D_6$ curves. Then we can plot the curves define by $D_8$=0… and so forth until we have mapped out the curves in the ranges we wish to show. This same procedure can also be used to plot out the curves defined by the other three sequences; the result of this is shown in Figure 5.2.

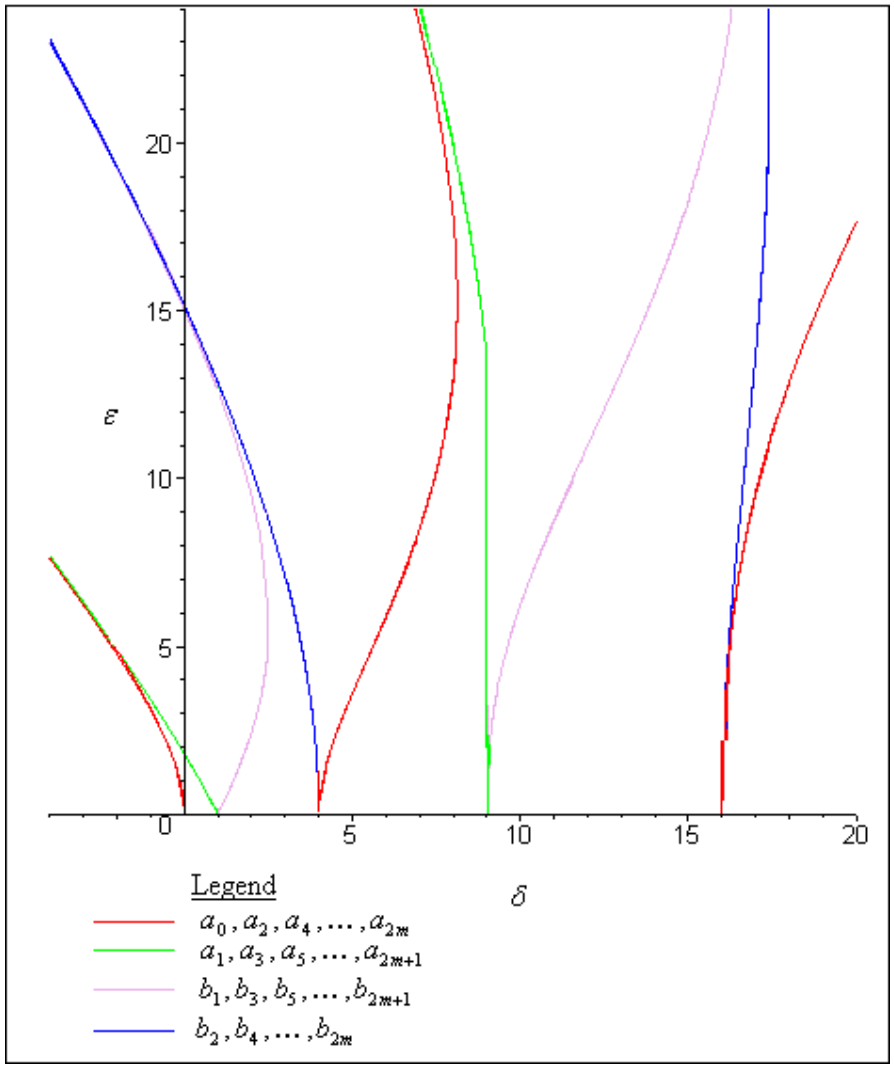


Figure 5.2. The curves defined by determinate sequences.

Figure 5.2 shows the curves define by the determinants of the matrices and the legend shows to which sequence the curves are defined from. Note that the graph in Figure 5.2 is symmetric in the $\delta$-axis so only the positive section is shown. Remember that the even subscripts relate to solutions with a period $\pi$ (when $\phi = 1$) and the odd subscripts relate to solutions with a fundamental period of $2\pi$ (when $\phi = -1$). Also the curves continue along the $\delta$-axis indefinitely, growing out of the square numbers, so we only show a small section of the whole picture.

Notice that the stability boundaries arise from the points (when $\varepsilon = 0$) at the points defined by (5.31). Also recall that these are the only points about which unstable regions can be centred, and anywhere else along this axis there are stable solutions for (5.22). Because of this we know which regions given stable solutions of Mathieu's equation and the regions that are unstable. Figure 5.3 is a graph showing the regions of stability for the Mathieu equation (given by 5.22).

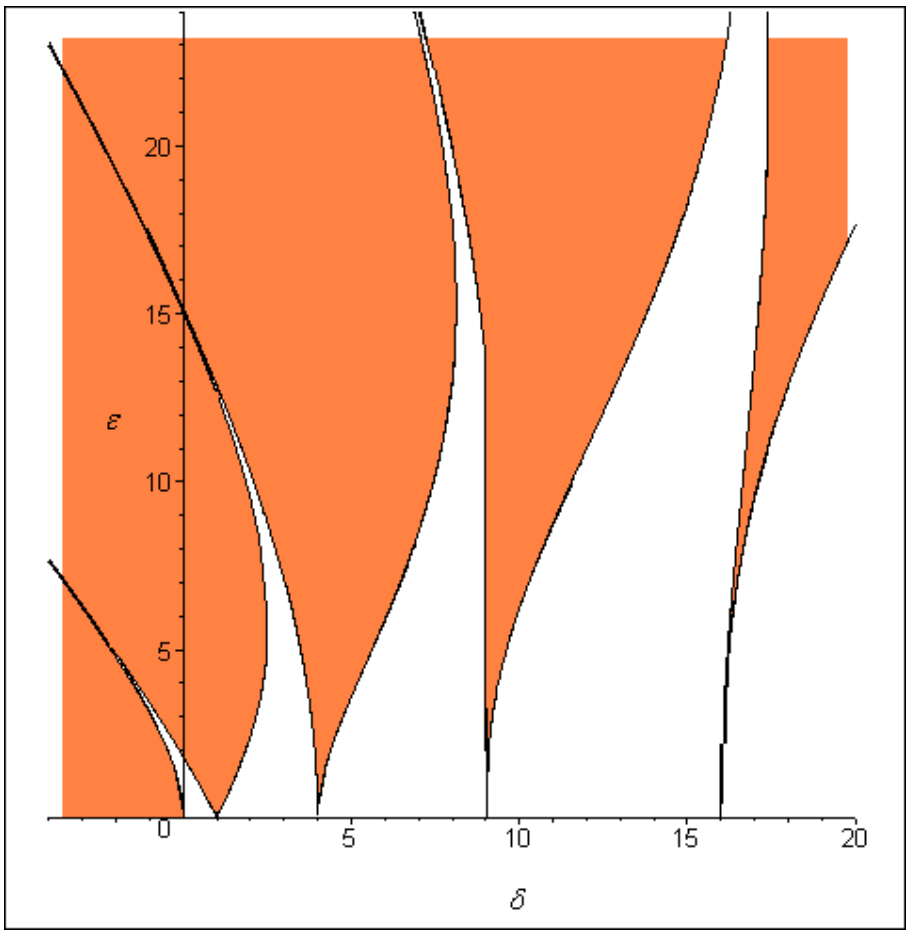


Figure 5.3. The stability regions of the Mathieu equation.

Here shaded regions relate to unstable solutions.

From Figure 5.3, we can see that as $\varepsilon$ increases these regions of stability become very thin.

### 5.4 Stability of the Inverted Pendulum

Now we have computed the stability regions of the Mathieu equation, we can now link this back to our inverted pendulum. Recall that the equation of motion for a pendulum with a vibrating pivot was given by

$$\frac{d^2\alpha}{dt^2} + k\frac{d\alpha}{dt} + \left(\frac{g}{l} + \frac{a\omega^2}{l}\cos(\omega t)\right)\sin(\alpha) = 0\,. \tag{5.48}$$

We commented at the end of section 4.1 that it was possible to take away the air resistance and the pendulum still remains inverted. Therefore it is reasonable for us to begin analysing the stability of the inverted pendulum using a simpler equation omitting the resistance, hence (5.48) becomes,

$$\frac{d^2\alpha}{dt^2} + \left(\frac{g}{l} + \frac{a\omega^2}{l}\cos(\omega t)\right)\sin(\alpha) = 0\,. \tag{5.49}$$

If we look at a diagram of the inverted pendulum (as in Figure 5.4), we see that it is essentially the same as the diagram of the pendulum with a vibrated pivot from section 4 (Figure 4.1) but upside-down. Hence the only change is that the acceleration due to gravity is now in the opposite direction (i.e. $g$ becomes $-g$), see figure below.

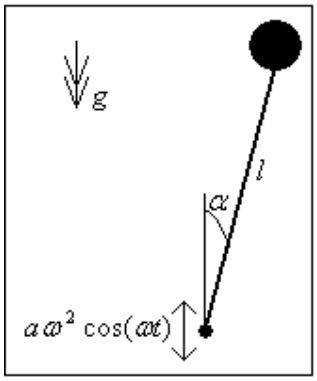


Figure 5.4. The inverted pendulum with a vibrating pivot.

Therefore, whereas in (5.48) for a stable inverted position we would require $\alpha \to \pi$ as $t \to \infty$, we could rewrite (5.48) as,

$$\frac{d^2\alpha}{dt^2} + \left( -\frac{g}{l} + \frac{a\omega^2}{l}\cos(\omega t) \right) \sin(\alpha) = 0 , \tag{5.50}$$

and then require $\alpha \to 0$ as $t \to \infty$ for a stable inverted position. Also notice that since $\alpha$ is measuring deviations from the upward vertical, for a *stable* inversion we can use the simplification,

$$\sin(\alpha) = \alpha .$$

Equation (5.50) now becomes,

$$\frac{d^2\alpha}{dt^2} + \left( -\frac{g}{l} + \frac{a\omega^2}{l}\cos(\omega t) \right) \alpha = 0 . \tag{5.51}$$

Equation (5.51) is now in a form similar to Mathieu's equation. Recall that Mathieu's equation was given by,

$$u'' + \left(\delta + \varepsilon\cos(2t)\right)u = 0 \tag{5.52}$$

Let us introduce the scaling $2\tau = \omega t$ into (5.51) {and divide through by $\omega^2/4$ since this is a non-zero term}, this then becomes,

$$\frac{d^2\alpha}{d\tau^2} + 4\left(-\frac{g}{l\omega^2} + \frac{a}{l}\cos(2\tau)\right)\alpha = 0 \qquad (5.53)$$

Now we can use what we know about the stability of Mathieu's equation on (5.53).

If we then equate the relevant parts of (5.52) and (5.53) we find that,

$$\delta = -\frac{4g}{l\omega^2} \qquad \text{and} \qquad \varepsilon = \frac{4a}{l} \qquad (5.54)$$

Because $g$ and $l$ are both positive constants we can see from (5.54) {recall that we wish to find $\omega$} that the area of Figure 5.3 that we are interested in is when $\delta$ is negative, this section is shown enlarged below in Figure 5.5.

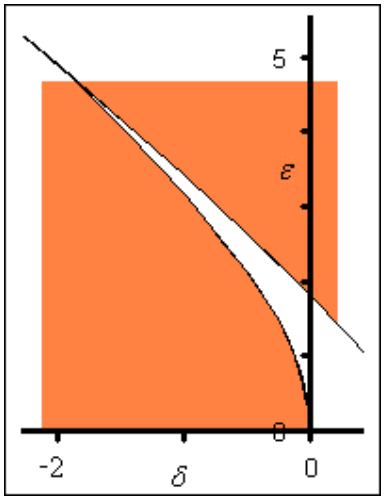


Figure 5.5. The stability boundaries of the Mathieu equation for $\delta$ negative.

If we then use the equations given by (5.54) we find,

$$\frac{\omega}{(g/l)^{1/2}} = 2\sqrt{-1/\delta} \qquad \text{and} \qquad \frac{a}{l} = \frac{\varepsilon}{4} \qquad (5.55)$$

We can then use the points on the curves in Figure 5.5 substituted into (5.55) to find the stability boundaries of the inverted pendulum (without air resistance). The result of this is shown in Figure 5.6.

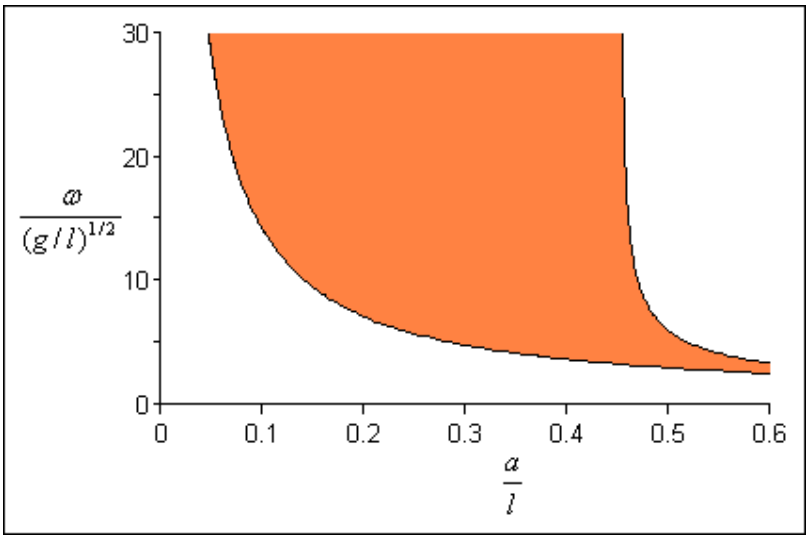


Figure 5.6. The region of stability for the driven inverted pendulum (with no air resistance). The shaded region relates to a stable inverted state.

Our analysis thus far has involved us neglecting air resistance on the pendulum. We notice that when the inverted pendulum is indeed stabilising there is little 'swinging' motion. Also Acheson (2003, page 175) notes that adding in damping merely "erodes the sharp tips of the instability regions", so we can expect that Figure 5.6 is a good representation of the stable region for the driven inverted pendulum.

# 6. Practical Demonstrations

## 6.1 Computer simulation

Accompanying this report is a CD. On this disk is two folders labelled 'Excel Worksheets' and 'Maple Worksheets'. They include examples of worksheets that I have used throughout this project. All the labels and parameters ($\alpha$, $h$ etc) are consistent with those used throughout this report.

One of the Excel sheets is labelled 'Interactive worksheet'. This worksheet has two pages; one for a single pendulum and one for a double pendulum. Let us take the single pendulum as an example. The worksheet starts with the box in Figure 6.1.

| | |
|---|---|
| h= | 0.01 |
| Initial Angle= | 3.141493 |
| Initial Speed= | 0 |
| Gravity= | 9.8 |
| String Length= | 9.8 |
| k= | 0.1 |
| a= | 1 |
| drive frequency= | 10 |

Figure 6.1. A section of the Interactive Excel worksheet.

It is possible to change any of the values in the blue boxes, and upon pressing enter the graphics should change to reflect this 'new' pendulum motion.

The Maple worksheets are a little more interesting. As well as creating graphs such as phase paths that have been used in this project, I have also included some animation on most of the worksheets. To see these animations simply open up the worksheet and scroll down to the last picture. For example on the 'dancing pendulum' worksheet the last picture looks like Figure 6.2 below.

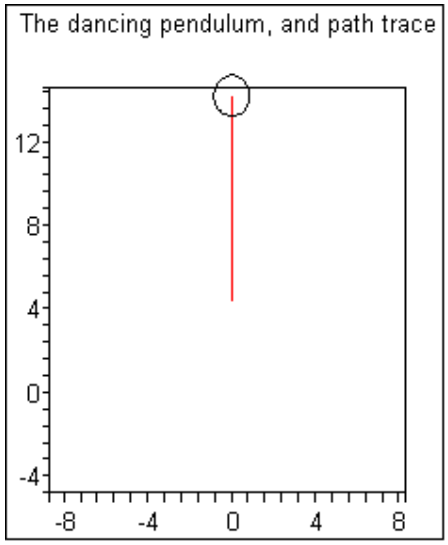


Figure 6.2. The dancing pendulum animation.

Once the image has been clicked on some new 'buttons' should appear in the Maple tool bar. In Maple 9.5 the new tool bar is that of Figure 6.3.

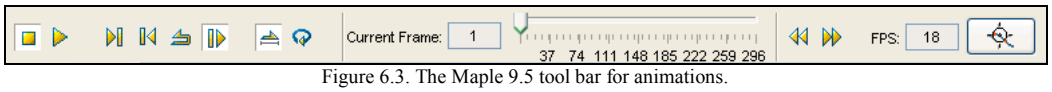


Figure 6.3. The Maple 9.5 tool bar for animations.

Press the right pointing arrow (the play button) to make the animation move. The double pendulum with a vibrating pivot is recommended viewing. As with the Excel worksheets, all the values can be changed to show different pendulum motion. The

user needs to click on the !!! button once they have changed the parameters for the Maple worksheet to rerun itself.

### 6.2 A working model

In section 5.4 we discovered the parameter values for the vibrating pivot that would enable a (single) pendulum to remain in a stable upright position (Figure 5.6). We now test this theory in the practical world. I chose the rod length of the pendulum to be 19cm. Figure 6.4 is computed from Figure 5.4, and shows the parameter values for which we need to vibrate the pivot in order to maintain the stable inverted position.

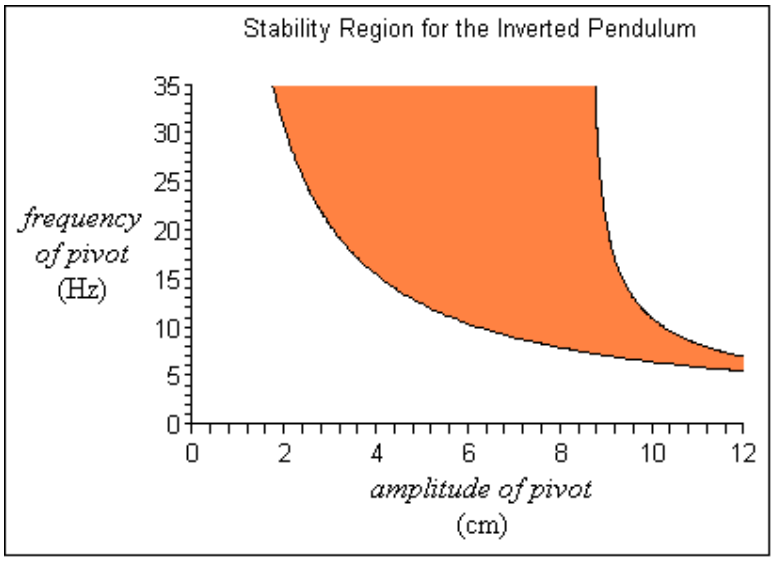


Figure 6.4. The stable region of the inverted pendulum for the vibrating pivots parameters.

The rod for the pendulum was made of stainless steel tubing because it is rigid and light and hence consistent with the assumptions made early in the report. The bob of the pendulum was made of a pivot joint (to which we could a join on another

pendulum) and was about 50 grams. The set-up of the experiment can be seen in Figure 6.5.

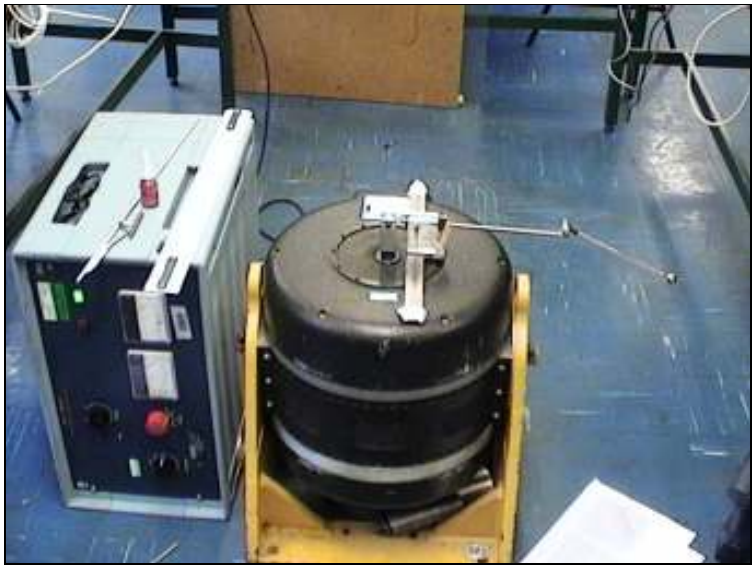

Figure 6.5. The set-up of the inverted pendulum experiment.

The black drum in the middle of Figure 6.5 is a ‘shaker’. In the centre of the top of the shaker is a pin that vibrates up and down with a frequency and amplitude controlled by the box on the left of the picture. Initially the pendulum was connected directly onto this pin, but we were unable to generate the required amplitude at the frequencies we needed so we built a simple seesaw to increase the amplitude.

The initial plan of the experiment was to try different values in order to pick out one of the curves defined in Figure 6.4. However, the shaker was not as reliable as I hoped and we were unable to obtain accurate readings for the amplitude and the frequency. We were able to see the stable inverted state, a picture of this can be seen below in Figure 6.6.

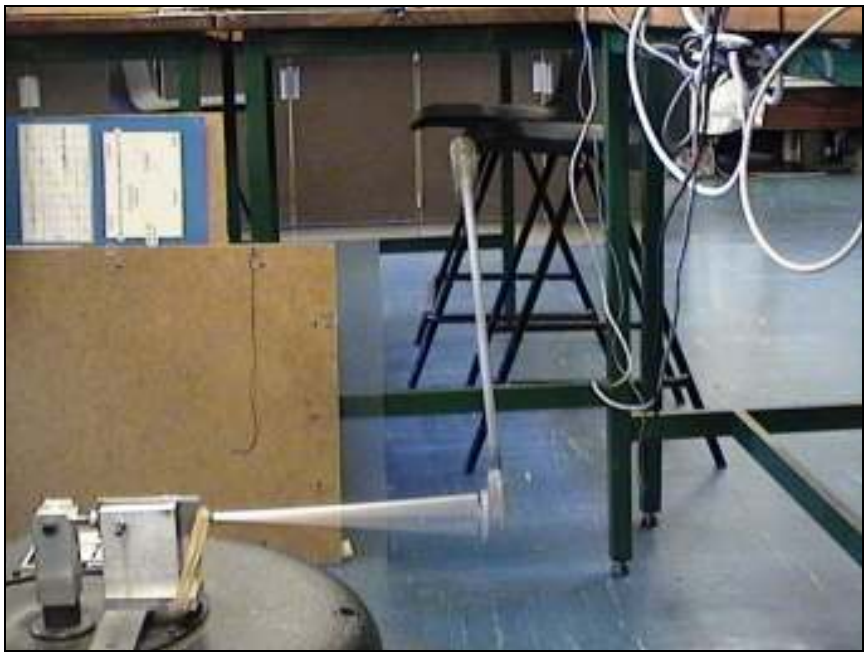

Figure 6.6. The stable inverted pendulum.

The pivot for the pendulum in Figure 6.6 was vibrated about 3cm at about 33Hz. The inverted state was very stable, and we were able to tilt the pendulum about 45 degrees away from the inverted position and it would self-right within a couple of seconds. A video of this experiment is included on the CD.

Although we did not cover the theory for the inverted double pendulum as rigorously as for the single inverted pendulum in this report, we did join a double pendulum to our rig. The inverted double pendulum can be seen in Figure 6.7.

Figure 6.7. An inverted double pendulum.

Observant readers may notice that our ‘see-saw’ rig is slightly different in Figure 6.7 than in Figure 6.6. The reason for this is that on the first trial for the double pendulum the rig became very heated (due to the higher frequency needed to invert the double pendulum as apposed to a single pendulum) and snapped at the point where it was connected to the shaker. We built a new rig with a more solid piece of metal at this weak point. We then managed to invert the double pendulum with this new rig. Our new rig also did not survive the experiment but did last long enough for a small piece of film footage that is included on the CD. (The collapse of the double pendulum in film is due to the new rig breaking, this time in the centre of the seesaw). The new rig broke before we could obtain figures for the pivot amplitude and frequency.

# Appendix

**Appendix Contents**

**A1. Reviews of initial research resources.**

ACHESON, D., 1997. *From Calculus to Chaos, An Introduction to Dynamics*. New York: Oxford University Press Inc.

On the back cover of the book it is written:

"David Acheson's book will inspire new students by
showing how remarkable and interesting the
applications of mathematics can be."

I feel this is a perfect description for the book. The book covers a wide area that is needed to understand, set up and solve dynamical systems. Acheson writes enthusiastically and in a style that is clear to understand. Throughout the whole book he demonstrates the ideas and theories with demonstrations, and all the computer work is included, even an appendix that enables the reader (with no programming experience) to try the examples on their own computer.

HANNAH, J., and HILLER, M J., 1995. *Applied Mechanics*. 3rd Edition. Longman Scientific and Technical.

On the back cover of this book it is described as:

"..the essential guide to the basic
principles of applied mechanics…"

Again I feel this is an accurate description of the contents. The two authors cover an extensive range of topics, incorporating all areas of mechanics. Not only was is book useful in setting up equations for any particular project, it is written in a way that encourages the reader to continue and discover about

other forms of mechanics. Included in the book are a very large number of useful illustrations that help to explain the text

ROTT, N., 1970. *Zeit. Angew. Math. Physik*. Vol. 21, pp. 570-582.

The journal paper is intensely complicated to understand. However after a few times of reading it is an interesting look at coupling effects. The main area of discussion is a special 'tuning' (as he refers to it as) in which a coupling effect (usually a weak force) becomes strong. Coincidently, this source is referred to in Acheson's book (which I received after).

*Tomorrow's World*, 1995. TV, BBC1. Oct 27.

I contacted the BBC after David Acheson referred to this source. We do get to see the experiment of the inverted triple pendulum performed in the episode. The experiment, preformed by David Acheson and Tom Mullin, is successful and interesting to watch. They then go on to demonstrate that the same effect can be achieved with a piece of wire instead of pendulums, which prompts the presenter to make and analogy to the Indian rope trick. The only criticism of this source is that the experiment was not the main topic of the program and as such was only concentrated on for a few minutes, but what featured was interesting.

A list of all the sources I have used so far is completed at the end of this report, the above reviews were the key resources to get me started with the project.

**A2. Iterative schemes applied to the equation of motion for a single pendulum with no damping.**

The system of equations used to model the motion of the pendulum was given by equations (2.24), which were

$$\frac{dz}{dt} = -c^2 \sin(\alpha),$$
$$\frac{d\alpha}{dt} = z.$$

The Euler iterative scheme is given by,

$$z_{n+1} = z_n - hc^2 \sin(\alpha),$$
$$\alpha_{n+1} = \alpha_n + hz_n,$$
$$t_n = t_0 + nh,$$

where $n$ relates to the $n^{\text{th}}$ iteration, and $h$ is the step size (in this case how far in time we proceed) between iterations.

The Modified Euler iterative scheme is given by,

$$z^p{}_{n+1} = z_n - hc^2 \sin(\alpha_n),$$
$$\alpha^p{}_{n+1} = \alpha_n + hz_n,$$
$$t_n = t_0 + nh,$$
$$z_{n+1} = z_n - \frac{1}{2} hc^2 \left[\sin(\alpha_n) + \sin(\alpha^p{}_{n+1})\right],$$
$$\alpha_{n+1} = \alpha_n + \frac{1}{2} h\left[z_n + z^p{}_{n+1}\right].$$

The iterative scheme above is a predictor-corrector scheme. This means that it predicts the next value and then uses this prediction to calculate a more accurate *correct* value, $p$ relates to this predicted value.

## A3. The iterative scheme used to solve the equation of motion of a damped pendulum

The system of equations modelling the motion of a damped pendulum was given by,

$$\frac{dz}{dt} = -kz - c^2 \sin(\alpha),$$
$$\frac{d\alpha}{dt} = z.$$

The Modified Euler iterative scheme used to solve this system is given by,

$$z^{p}{}_{n+1} = z_n - h\left[kz_n + c^2 \sin(\alpha_n)\right],$$
$$\alpha^{p}{}_{n+1} = \alpha_n + hz_n,$$
$$t_n = t_0 + nh,$$
$$z_{n+1} = z_n - \frac{1}{2}h\left[kz_n + c^2 \sin(\alpha_n) + kz^{p}{}_{n+1} + c^2 \sin(\alpha^{p}{}_{n+1})\right],$$
$$\alpha_{n+1} = \alpha_n + \frac{1}{2}h\left[z_n + z^{p}{}_{n+1}\right].$$

## A4. Altering parameters of a damped pendulum

*Initial Angle*

Figure A.1 shows the difference in motion when the initial angle was changed from that of 0.2 radians to 0.1 radians.

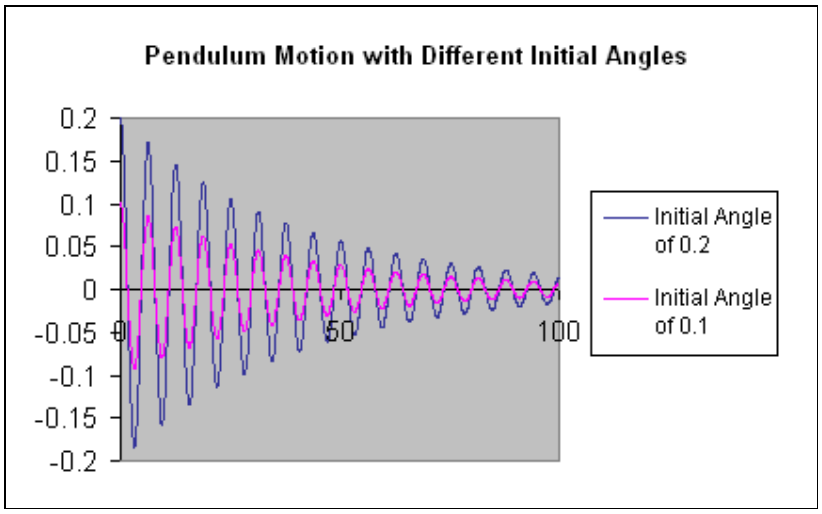


Figure A.1. The motion of two pendulums with only the initial angle differing.

We can see from the graph that the frequency of the two pendulums is the same. The difference between the pendulums is the amplitude. At each point we can see that the pendulum with an initial angle of 0.2 radians swings with an amplitude twice that of the pendulum with an initial angle of 0.1 radians.

We can see that this would be the case for the model for *small* angles of the pendulum that was not damped. Equation (2.19) shows us that the amplitude will be equal to the initial angle, but we can see from the graph that for *all* examples the initial angle is the factor affecting the amplitude.

*Damping Effect*

One of the variables we introduced was for the damping effect. Figure A.2 shows two pendulums subject to different amounts of resistance.

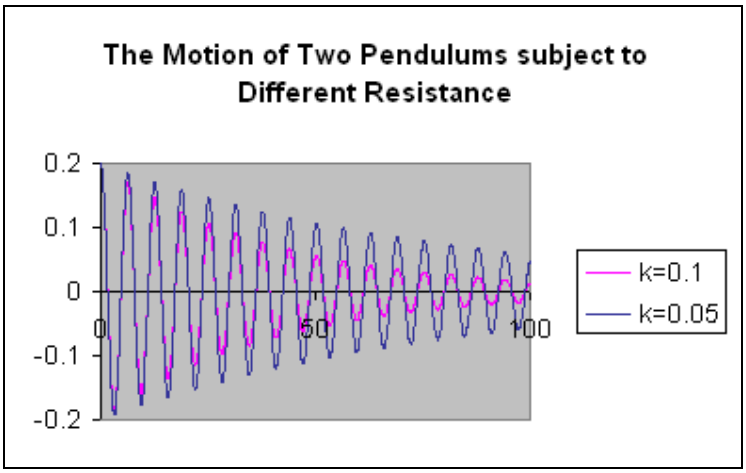


Figure A.2. The motion of pendulums with different damping effects

Figure A.2 shows that as the resistance increases the pendulums amplitude decreases. The resistance appears not effect the frequency of the pendulum, only how far it swings. This is an intuitive effect we see in the real world.

*Length of the String*

In section 2.2 we discovered that the period, and hence frequency, was effected by the length of the string only. Figure A.3 shows two pendulums with different length strings.

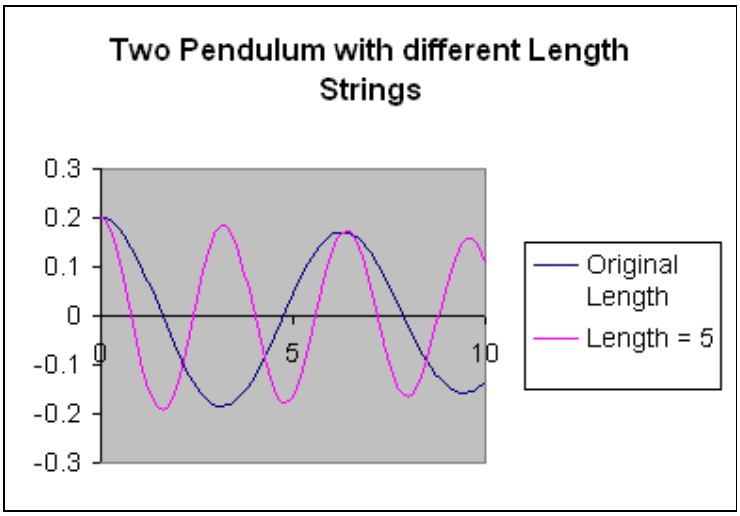


Figure A.3. Demonstration of changing the length of string for a pendulum

Up to this point in the project the length of the string was scaled such that $c^2 = 1$. The other pendulum in Figure A.3 has a shorter length of 5 metres. (It is important to note that making the length of the string shorter has the same effect of increasing gravity by the same factor, this can be seen by the ratio of Equation 2.9).

From the graph we can see that the length of the string does indeed affect the frequency of the pendulum. We can see that the longer length pendulum takes longer to complete the swinging action. This effect is used in making pendulum clocks, if the clock is running slow the pendulum can be raised.

*Step Size*

We can use the investigation so far to examine the Improved Euler's Method. The iterative process depends on the step-size. In terms of this project this means how far in time we move before calculating the positions of the pendulums based on the last position. Up until now the step-size used was 0.1 seconds.

Because iterative methods rely on previous results to calculate future positions, the smaller the 'jump' between estimations the more accurate the results will become. When raising the step-size slightly for this project the graph did not seem to move noticeably, this is because I have chosen a small step-size to obtain accurate results. However, if we take a step-size much greater (in this example six time greater) we can see how different the results could be due to the increase in error of the iterative process.

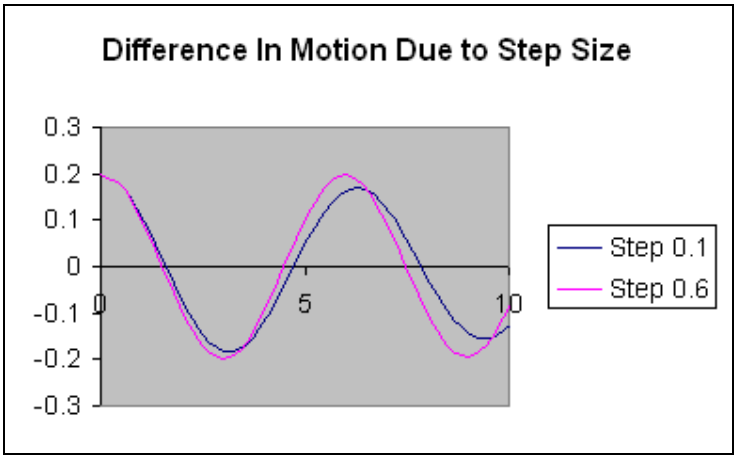


Figure A.4. Example of changing the step size in the Improved Euler's Method

Figure A.4 is the graph showing the same pendulum motion estimated with a small accurate step-size and then an inaccurate large step-size. If we look closely at the motion described with a step-size of 0.6 seconds, it appears that the pendulum swings with an increasing angle each time instead to a decreasing angle. Therefore it is important to realise if we wish to use a higher step size we should use methods that have a smaller global error.

It is for this reason we now choose to use an even more accurate method than Modified Euler's method. Whilst a global error proportional to $h^2$ has given us good results up until now, in the 'real world' methods of accuracy of order $h^4$ are more appropriate when $h$ is given typical value of 0.1. From now on I will use the classical fourth order Runge Kutta scheme. This means we can now achieve more accurate results without having to make more calculations.

# Bibliography

**Books**

ACHESON, D., 1997. *From Calculus to Chaos, An Introduction to Dynamics*. New York: Oxford University Press Inc.

GRIMSHAW, R., 1990. *Nonlinear Ordinary Differential Equations*. Blackwell Scientific Publication.

GLENDINNING, P., 1994. *Stability, instability and chaos: an introduction to the theory of nonlinear differential equations*. Cambridge University Press

HANNAH, J., and HILLER, M J., 1995. *Applied Mechanics*. 3rd Edition. Longman Scientific and Technical.

JACQUES, I., and JUDD, C., 1987. *Numerical Analysis*. London: Chapman and Hall Ltd.

JORDAN, D W., and SMITH, P., 2002. *Mathematical Techniques*. 3rd Edition. New York: Oxford University Press Inc.

JORDAN, D W., and SMITH, P., 2004. *Nonlinear Ordinary Differential Equations; An introduction to Dynamical Systems*. 3rd Edition. Oxford University Press.

McQUARRIE, D A., 2003. *Mathematical Methods for Scientists and Engineers*. California: University Science Books.

**Internet Sources**

ANON., *Double Pendulum* [online]. Available at <http://www.yorku.ca/marko/ComPhys/DblPendulum/DblPendulum.html> [Accessed June 07, 2004].

BANNISTER, R., *The Double Pendulum* [online]. Available at <http://www.met.rdg.ac.uk/~ross/Physics/DPl.html> [Accessed June 07, 2004].

WEISSTEIN, E,. *Eric Weissteins's World of Physics* [online]. Available at <http://scienceworld.wolfram.com/> [Accessed June 07, 2004].

**Television Documentaries**

*Tomorrow's World*, 1995. TV, BBC1. Oct 27.

**Mathematical Papers**

ACHESON, D., 1993. *Proceeding of the Royal Society*. Vol 443, pp. 239-245.

ACHESON, D., 1995. *Proceedings of the Royal Society*. Vol 448, pp. 89-95.

ROTT, N., 1970. *Zeit. Angew. Math. Physik*. Vol. 21, pp. 570-582.

STEPHESON, A., 1908, *Philosophical Magazine*. Vol 15, pp.233-236.

STEPHESON, A., 1908, *Proceedings of the Manchester Literary and Philosophical Society*. Vol 52, Pt 8, pp. 1-10.

STEPHESON, A., 1909. *Philosophical Magazine*. Vol 17, pp. 765-766.